

MAGNETIC ASYMMETRY AND FLUCTUATIONS OF THE
GENERAL MAGNETIC FIELD OF THE SUN

BY A. B. Severnyy

From: Akad. Nauk SSSR, Izvestiya Krymskoy Astrofiz. Observ., v.38,
1967, p.3-51.

Translated by
Belov & Associates
for
N.A.S.A. GSFC Library
Contract NAS 5-10888
Item no. 10888-017
November 1969

FACILITY FORM 602

N70-73951 _____ (THRU)
(ACCESSION NUMBER)

90 _____ (CODE)
(PAGES) *None*

CR-110071 _____ (CATEGORY)
(NASA CR OR TMX OR AD NUMBER)



Magnetic Assymetry and Fluctuations of the General Magnetic Field of the Sun

The influence of magnetograph resolving power on the statistical results of the mean intensity \bar{H} , the length $\bar{\lambda}$, and the number π of "magnetic elements" (of different polarity) of the general magnetic field of the sun has been investigated. It was found that, while the net magnetic flux and \bar{n} remain constant, the mean field strength (of a given sign) increases by a factor of 1.3 - 1.4 (Table 3), and the length $\bar{\lambda}$ decreases by a factor of 1.2 - 1.3 when resolution is increased from 27" to 2.5" (c.f. Table 4, Fig. 2). It was also found that at a resolution of 23" X 23" (Mount Wilson routine recordings), about 50% of all the general magnetic field components with a length of less than 10" were not recorded (below noise level), while according to the Crimean routine recordings of the field, less than 10% of the components with a magnitude of less than 3" are lost (resolution, 2.5" X 9").

Twenty-four (24) recordings of the N- and S-polar regions (latitude 55 - 75°, longitude \pm 25°, cf. Table 1), made in 1965, were measured and analyzed by the very same method as in ref. [1]. Although the total histogram (Table 5, Fig. 10) for the whole year indicates that in 1965 the sun was very nearly dipolar with a new field of +0.6 gs (S-polarity) at the north and -0.8 gs at the south, there were sharp deviations from this activity (cf. Fig. 11). Slow fluctuations, most prominent in September - October, 1965, were discovered when both polar regions were of the same S-polarity. Most interesting

five rapid (on the order of 1 day) fluctuations, almost synchronous at both poles, which always exhibit a lapse (on the order of 24 hours) of the northern peak behind the southern peak (cf. Fig. 11, which also gives the Mount Wilson data). Just as in 1964, there was a flux bias of the southern polarity at the north pole over this same flux at the south pole, and over fluxes at poles of opposite polarity (cf. (3.4) for mean flux ratios) - an effect due to the great expanse of the magnetic field substantiates these conclusions and indicate that the field in the chromosphere is ~ 1.5 times less (weaker) than in the photosphere.

A study of five magnetic field recordings of the entire (solar) disk, made at high resolution (cf. Fig. 13), showed that (for a given latitude) the distribution of mean flux ($F_S - F_N$) was non-uniform over the whole disk (cf. Fig 14), which sometimes leads to the magnetic asymmetry effect - a bias of one polarity in the northern and southern hemispheres, and even throughout the entire (solar) disk (df. Table 8). The net flux from the visible hemisphere of the sun varies from $+8.10^{21}$ to -9.10^{21} Mxv: reasons are set forth as to why these fluctuations, as well as polar field fluctuations, could hardly be connected with rotation of the sun.

Auto-correlation curves (cf. Fig. 17) for general magnetic field strength fluctuations were in good agreement with those found by Rogerson for intensity fluctuations of the Ca^+ -chromosphere grid. The radius of auto correlation (7.5"), as well as the position of the principal maximum on the "magnetic component" size histogram,

indicates that 50 - 60% of the elements (components) are shorter than 12". Two weak secondary maxima on the histogram (24" X 48") indicate, as in ref. [1], the possibility of steady fluctuations with two overtones. There also exists a well expressed cross-correlation between magnetic fields at different photosphere levels (λ 5250 & λ 6103 Cu I), but practically no type of correlation between field fluctuations at these levels and the corresponding radial velocities.

1. Observational Data. Comments on Methodology

This paper is part of a series of investigations of the general magnetic field of the sun, beginning with the period, 1963 - 1964 [1]. Data on registrations of the general magnetic field during 1965 and the first of 1966 are compiled in Table 1. As a rule, recordings were made of the S- and N-polar zone sections which extend over α at $\pm 120''$ from the right, joining the north and south points on the disk, and over δ , 30" to 180" from the N- or S-limbs of the disk (which corresponds to latitudes from 76 - 54°). Scanning of this rectangular section was carried out over a radian angle δ , at 30" intervals; scanning speed was 1" per sec of time ($v = 30$, 15 March, 1965, with part of the recording made at $v = 60$, i.e., 1"/sec); and the time constant was 2.5^s. In five cases (Table 1), when the weather was still and cloudless the entire day, recordings of the complete disk were made (from W to E). In this case, it was necessary to scan at a rate twice as fast (2"/sec) and the distance between successive sections was doubled, i.e. 60" in order to record the entire disk within a day (8 - 10 hrs.).

The principal difference between the method used in [7] and in this work and the method used by Babcock [2] is that the resolving power of our recordings (usually, 2" X 9", and sometimes 2" X 4.5") was 10 times higher than in [2] and \sim 30 times higher than in the daily recordings at Mount Wilson Observatory (23" X 23"). Although the resolution of our recordings was inferior to that of Leighton's spectroheliographic method [3], which depended solely upon manifestations of solar activity, the method employed in [3] does not permit detection of those weak fields < 30 gs, which constitute the major part of the general field. Therefore, this method is unsuitable for investigating the general field due to the substantial loss of information.

A second important difference from all previous work on the general field, including our first study [1], is that recordings of the field for 1965 - 1966 were made not only at the green line λ 5250, but also at other lines, e.g. $H\alpha$ or λ 6103 Ca I; from 10 August, 1965, similar recordings were made simultaneously with two magnetographs as described in [4]. Such simultaneous recordings are of special interest in understanding the nature of the general solar magnetic field. They also facilitate considerable increase in the number of recorded deflections, which are caused by the field and which are distorted against a noise background: fluctuations, caused by the field are lost on recordings at both lines in one and the same place. In Section 4 the general magnetic field at the chromosphere level is reviewed according to $H\alpha$ line recordings.

Table 1. Observational Data

1	2	3	$\lambda, \text{\AA}$	4	5	6	7	8	9	10	11
1	24.I 1965 № 399	13 ^h 00 ^m —15 ^h 05 ^m	5250	400	60×1,5	13 ^h 00 ^m	172	2000	2,0	$N_{0,5}-N_{3,0}$ $S_{0,5}-S_{3,0}$	0,50
2	12.II № 402	12 20 —14 15	5250	400	60×1,5	12 20	133	2000	2,40	$N_{0,5}-N_{3,0}$ $S_{0,5}-S_{3,0}$	1,22
3	15.III № 403	12 00 —16 30	5250	400	60×1,0	11 45	210	2000	1,52	$N_{0,5}-N_{8,0}$ $S_{0,5}-S_{8,0}$	
4	16.III № 403—404	10 30 —17 14	5250	400	100×1,5	9 50	210	2000	1,52	$N_{1,0}-N_{14,0}$ $S_{1,0}-S_{14,0}$	
5	17.III № 405	14 30 —17 00	5250	400	100×1,5	14 30	171	2000	1,87	$N_{0,5}-N_{4,5}$ $S_{0,5}-S_{4,5}$	1,40
6	7.IV № 406a	11 00 —17 30		400	100×1,5	9 50	232	2000	1,38	$N_{1,0}-N_{12}$ $S_{1,0}-S_{12}$	
7	15.VI № 418	8 40 —11 10	5250	30 30	80×1,0	8 40	115 170	100 100	4,20 2,90 ср. 3,50	$N_{1,0}-N_{3,5}$ $S_{1,0}-S_{3,5}$	1,80
8	10.VII № 427	15 08 —16 30	5250	40	80×1,0	15 08	117	200	2,74	$N_{0,5}-N_{2,5}$ $S_{0,5}-S_{2,5}$	2,09
9	23.VII 1965r. № 436	12 ^h 00 ^m —13 ^h 25 ^m	5250	30	60×1,0	12 ^h 00 ^m	145	150	2,21	$N_{0,5}-N_{3,0}$ $S_{0,5}-S_{3,0}$	2,00
10	24.VII № 437	10 00 —11 10	5250	20	60×1,0	10 00	121	150	1,77	$N_{0,5}-N_{2,5}$ $S_{0,5}-S_{2,5}$	2,03
11	27.VII № 440	7 10 —19 18	5250	50	60×1,0	7 00	158	150	3,30	$N_{0,5}-N_{14}$ $S_{0,5}-S_{14}$	—
						13 20	108	150	4,94 исключе- ние	$N_{4,5}, N_{7,5}, N_{8,0}$ $S_{4,5}, S_{7,5}, S_{8,0}$	
12	29.VII № 441	7 20 — 9 40	5250	20	60×1,0	7 20	113	100	2,84	$N_{1,0}-N_{4,0}$ $S_{1,0}-S_{4,0}$	1,96
13	31.VII № 443	16 20 —17 45	6103	30	80×1,0	16 20	97	300	1,10	$N_{0,5}-N_{3,0}$ $S_{0,5}-S_{3,0}$	1,87
14	1.VIII № 444	9 00 —10 10	6103	30	80×1,0	9 00	116	300	0,90	$N_{0,5}-N_{3,0}$ $S_{0,5}-S_{3,0}$	2,00
15	2.VIII № 445	8 15 —15 35	6103	50	80×1,0	8 10	162	300	1,05	$N_{1,0}-N_{15}$ $S_{1,0}-S_{15}$	—
16	10.VIII № 449	16 05 —17 00	5250	200	70×1,0	16 05	220×1,5	400	1,21	$N_{1,5}-N_{2,5}$ $S_{1,5}-S_{2,5}$	2,14

1) No. P/P; 2) Data; 3) Time (Moscow); 4) ATT Records; 5) Gap;
6) Calibration: Time (Moscow); 7) Calibration: Reject; 8) ATT
calibrations; 9) Unit H^r gs/mm; 10) Recorded Section; 11) Length
1 mm.

Table 1. (Continued)

1	2	3	λ, Å	4	5	6	7	8	9	10	11
17	11.VIII 1965 r. № 450	12 ^h 30 ^m —13 ^h 45 ^m	5250	200 200	70×1,0	12 ^h 20 ^m	98×1,5 185×1,5	1000 500	1,10 1,15		
18	12.VIII № 451	10 15 —14 20	5250	50 100	100×1,0	10 15 10 50	50×1,5 50×1,5	200 200	2,67		
									5,33		
				100		12 30	160×1,5	100	3,33		
19	5.IX № 462	10 55 —12 45	5250	300	80×1,0	10 55	113×1,5	800	1,76		
20	20.IX № 469	8 50 —10 33	5250	500	80×1,0	8 50	114×1,5	1000	2,34		
21	27.IX № 475	10 20 —11 10	5250	500	80×1,0	10 20	150×1,5	1000	1,78		
22	17.X 1965 r. № 483	12 ^h 05 ^m —13 ^h 25 ^m	5250	500	80×1,0	12 ^h 05 ^m	200×1,5	1500	0,90	$N_{0,5}—N_{3,0}$ $S_{0,5}—S_{3,0}$	2,66
23	04.XII № 496	12 40 —13 30	5250	600	80×1,0	12 40	165×1,5	2000	0,965	$N_{0,5}—N_{2,5}$ $S_{0,5}—S_{2,5}$	0,66
24	13.III 1966 r. № 499	11 30 —18 10	5250	600	1) 80×1,0 2) 80×1,0	10 30 15 30	1) 208 2) 169	3000 3000	1,54 1,89	1,71	$N_{1,0}—N_{14}$ $S_{1,0}—S_{14}$
	13.III № 499	11 30 —18 10	6103	10	80×1,0	10 30 15 30	1) 143 2) 170	30 30	3,56 2,99	3,28	$N_{1,0}—N_{14}$ $S_{1,0}—S_{14}$

1) No. P/P; 2) Data; 3) Time (Moscow); 4) ATT Records; 5) Gap;
 6) Calibration: Time (Moscow); 7) Calibration: Reject; 8) ATT
 calibrations; 9) Unit H_{rr} gs/mm; 10) Recorded Section; 11) Length
 in mm.

Table 1. Notes by number

- 1 - $\tau = 5^S$, $v = 60$; field is also recorded on the disc center.
Calibration E - W = 1600, 10 August, 1966. Group 66 on E.
- 2 - $\tau = 5^S$, $v = 60$. Smaller group 68, 69 in the N-hemisphere.
The whole disc, $d_{\odot} = 35$.
- 3 - $\tau = 5^S$, $v = 60$, 30. Group 76 in N-hemisphere. Extinguishes.
The whole disc, $d_{\odot} = 35$.
- 4 - $\tau = 2^S$, $v = 15$. Group 76 in N-hemisphere, extinguishes.
- 5 - $\tau = 5^S$, $v = 60$; No spots observed.
The whole disc, $d_{\odot} = 35$.
- 6 - $\tau = 2^S$, $v = 15$. No spots observed.
- 7 - $\tau = 2^S$, $v = 30$. New FEV, EMI. No spots observed.
- 8 - $\tau = 2^S$, $v = 30$. ADP modulation situated behind the gap. Bi-polar group 102.
- 9 - $\tau = 2^S$, $v = 30$; No spots observed.
- 10 - $\tau = 2^S$, $v = 30$. No spots observed.
- 11 - The whole disc $\tau = 2^S$, $v = 30$. No spots observed.
- 12 - $\tau = 2^S$, $v = 30$. No spots observed.
- 13 - $\tau = 2^S$, $v = 30$. Calibration 1.90 (E - W) = 2060, group 105,
a very weak spot.
- 14 - $\tau = 2^S$, $v = 30$. The same calibration as 31 July, 1965, No
spots observed.
- 15 - The whole disc, $\tau = 2.5^S$, $v = 15$. The same calibration, no spots
observed.

Table 1. Notes continued.

- 16 - Simultaneous recording H_{α} ; $\tau = 2^s$, $v = 30$; calibration for 5250 $1.5 (E - W) = 800$, starting with this day and to 13 Marcy, 1966. The commencement of simultaneous recording on a twin magnetograph, weak group 108.
- 17 - Simultaneous recording H_{α} ; $\tau = 2^s$, $v = 30$; group 108 disappears.
- 18 - Simultaneous H_{α} ; v and τ the same as 11 August, no spots observed.
- 19 - Simultaneous H_{α} ; τ , v are the same. Group 112 is dipolar.
- 20 - Simultaneous H_{α} ; τ , v are the same. No spots observed.
- 21 - Simultaneous H_{α} ; τ , v are the same, output gap 0.6×1.2 by error. Very small group 118, 119.
- 22 - Simultaneous H_{α} ; τ , v are the same, no spots observed.
- 23 - $\tau = 2^s$, $v = 30$. Second channel did not function. Very small spot 129.
- 24 - The whole disc, simultaneous recording in $\lambda 5250$ and $\lambda 6103$; $\tau = 2^s$, $v = 15, 7$.
- 25 - Simultaneous recording of intensity in the nuclear lines, ray velocity. Calibration $(E - W) = 1600$ for $\lambda 5250$; $1.35 (E - W) = 2060$ for $\lambda 6103$. Somewhat small, single spots 145, 146 in N- and S-hemispheres.

A third difference is that the signal registered by us was proportional to the size of the longitudinal field H_{\parallel} , while in [2] and in other studies [5], the recorded signal was proportional to $H_{\parallel} \times I$, where I is intensity; in which case, the effect of I may seriously alter the results at high resolution when recording the entire disk.

Of prime importance in recording the entire solar disk is establishing the correct zero position [1, p. 103]; in the absence of instrument alignment and polarization, the dark line (closed slit of the spectograph) fixes the zero position. When these factors are present, the position of the median noise line is not the same at the primary and secondary ADP crystals, and in general, does not correspond to the dark line. With each recording of the general field, photomultiplier noise at the secondary modulator must be recorded in order not to confuse noise with deflections resulting from a weak magnetic field which would appear to be forceful with respect to the slit, when recording fluctuations of a "calm field". The median line of such noise, in the absence of alignment, depends upon brightness and must correspond to the dark line. In not one of the 1965 recordings was a difference in the position of these lines found to extend beyond the limit of 0.5 gs, which is noticeably less than full noise amplitude.

Such is the complex nature of instrumental polarization effects. In 1964 [1] we regulated the zero position in recording fluctuations in the non-magnetic line $\lambda 5123$. The recording of noise (at the

ADP) in the continuous spectrum range also offers the possibility of fixing the true zero position by taking the "non magnetic" polarization effect into account. Shifts of the zero position relative to the dark line (or median noise lines in the case of a secondary modulator) arise due to various emission effects which lead to the filtering of linear polarization through the ADP circular polarization modulator at the main frequency (in an H_{\parallel} recording set-up [1]).

Whether or not the drift of $\frac{1}{2}\lambda$ proceeds not only to a double frequency, but also in some degree, to a main frequency, may be ascertained if a polaroid is placed before the ADP circular polarization modulator: with this, at the main frequency (when adjusting to record the longitudinal field H_{\parallel}), a signal occurs whose magnitude and sign depend upon the orientation of the attenuation axis of the polaroid.

Whether or not the signal is associated with scattered light may be determined if the spectograph is covered, the signal from the polaroid remains. It is most favorable to record this signal in the continuous spectra to avoid confusion with field effects, although any (continuous) field effect is negligibly small (in adjusting for H_{\parallel}) in comparison with the complete linear polarization signal from the polaroid, especially in the active region. Therefore, if during registration of the general field, these signals from the polaroid are recorded, and if their relationship to the instrumental polarization signals is known, then the zero position error can be evaluated. Examples of polaroid signal recordings are given in Fig. 1. It is difficult to observe the instrument polarization signal directly because it is

very weak; however, it can be done. It shows up as a noise deflection line extending from the zero line (dark) in the range where there is no field fluctuation (at the primary ADP); this deflection shows up equally well, both in the continuous spectrum or in line $\lambda 5123$, and also in the magnetosensitive line; but in the latter case, care should be taken to avoid magnetic field effects.

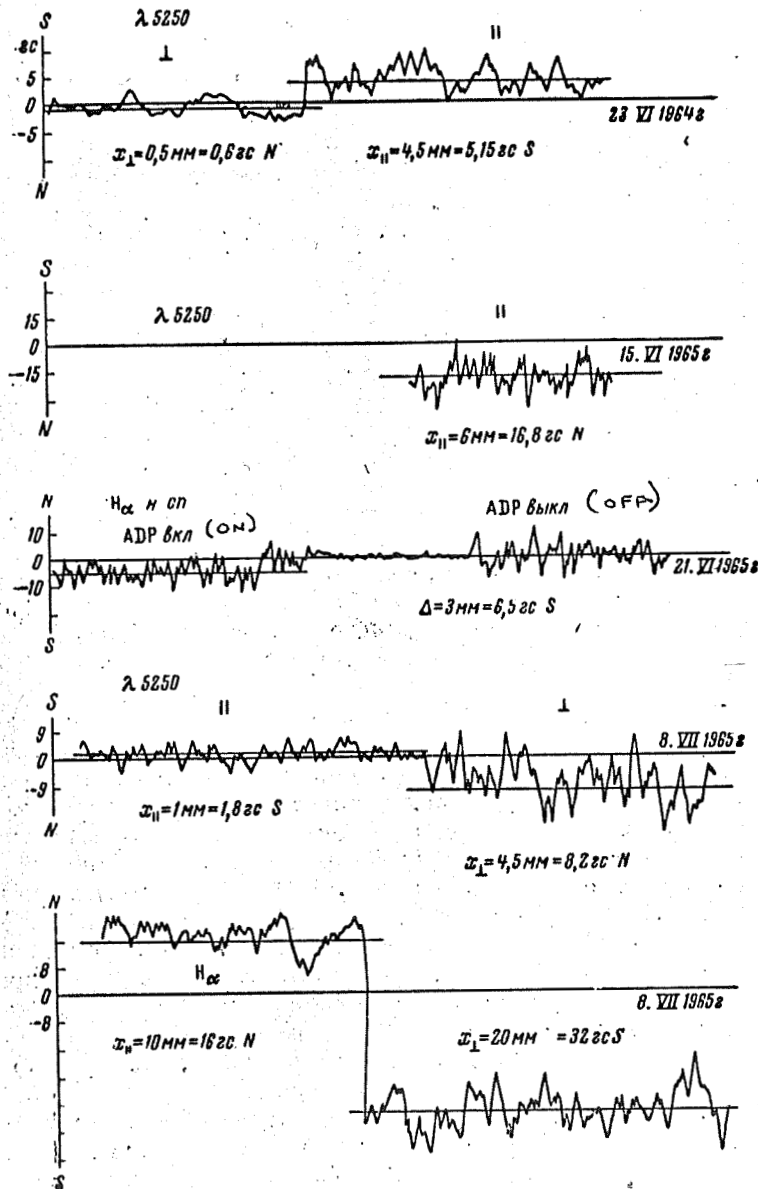


Fig. 1: Examples of linear polarization signal recordings with circular polarization modulator - a polaroid in front of the ADP with the attenuation axis parallel to (\parallel) and perpendicular to (\perp) the slit.

Table 2 gives some measurements of spontaneous zero shift relative to the dark line (with an indication of the direction of shift, i.e. to a N- or S-polarity), and also measurements of longitudinal fields signals from the polaroid with the axis of propagation along the slit, x_{\parallel} , and across x_{\perp} . From a comparison of these signals and the value Δ , it is obvious that Δ always has the sign x_{\parallel} and an average value of $\sim 1/16 x_{\parallel}$. As in [1], we find that in 1964, the zero shift may be disregarded, which follows also from control recording in $\lambda 5123$. However, upon resetting the magnetograph on dual for simultaneous recording in two lines [4], in May - June, 1965, scattered light augmented and made $\Delta \approx 1$ gs N for $\lambda 5250$. At the same time then, in May, upon setting up other multi-slit photomultipliers - EMI, an attempt was made to register the general field in H_{α} , which also showed a high instrumental polarization of 8:5N (noise in H_{α} , ~ 10 gs). This required radical improvement in arrangement, and in particular, removal of a powerful source of scattered light i.e., the ADP crystal located in or out of the spectrograph slit. On 23 June, 1965, an ADP modulator was installed behind the slit, which greatly improved its heat regime. Simultaneous removal of scattered light in the spectrograph by installing diaphragms in appropriate places required that (Table 2), for $\lambda 5250$ in 1965, the zero position corresponded to the dark line position (excluding apparatus adjustment periods when no recordings were made) with sufficient accuracy, i.e., at low noise amplitudes.

Table 2. Zero Position

Дата	$\lambda, \text{Å}$	$\alpha_{\parallel}, \text{sec}$	$\alpha_{\perp}, \text{sec}$	Δ, sec	$\frac{\alpha_{\parallel}}{16}, \text{sec}$
23.VI 1964 ¹	5250	5,15 S	0,6 N	—	0,32 S
1 15.VI 1965	5250	16,8 N	—	~1,0 N	1,05 N
2 21.VI 2	H $_{\alpha}$ (н. сп.)	135 N	—	6,0 N	8,5 N
3 8.VII 3	5250	1,8 S	8,2 N	<0,5 S	0,11 S
8.VII	H $_{\alpha}$	16 N	32 S	<5 N	1,0 N
19.VII	H $_{\alpha}$	34 N	21 S	<3 N	2,1 N
4 5.IX 1966 r.	5250	8,0 N	26,5 S	—	0,50 N
	6103	12,5 S	50 N	—	0,78 S
5 12.IX	5250	7,1 N	24,8 S	0,4 N	0,44 N
	6103	8,9 S	29,2 N	0,63 S	0,56 S

Comments by Number

1. With 20 May, 1965, new FEV, EMI and a reconstruction of the make-up.
2. 23 July, 1965. ADP situated behind the gap.
3. Declination values in H $_{\alpha}$ and λ 5250 correspond inversely to the right and left order of the grids (mesh).
4. In January - February, 1966, the schematics were reconstituted, 2nd channel for λ 5250.
5. 2nd channel for λ 5250.

The first recording of 1966 requires special consideration. 13 March, which is of considerable interest because it was made over the entire disk in two lines $\lambda 5250$ and $\lambda 6103$. Here, zero shifts, due to instrumental polarization during readjustment, must be considered in comparing results including both lines. If the deflection from the zero "dark" line is measured, then the entire recording in $\lambda 6103$ is shifted a bit downward, to the northern polarity, but the recording in $\lambda 5250$ is shifted upward to the southern polarity. This gives the systematic difference between the average field in the red and green lines $H_{\text{green}} - H_{\text{red}} = -2.3$ gs, counting the upward deflection (S-polarity) as positive. Since the actual value of $H = H_{\text{tr}} + \Delta$, where H_{tr} is the true field value (relative to true zero), and Δ is the zero correction; then counting H_{tr} for both lines simultaneously, we have $\Delta_{\text{red}} - \Delta_{\text{green}} = 2.3$ gs. While it follows from Table 2 that, on an average, on one hand $x_{\parallel}(\text{red})/x_{\parallel}(\text{green}) = -1.4$ and on the other hand, $\Delta_{\text{red}}/\Delta_{\text{green}} = -1.6$, so on an average, $\Delta_{\text{red}} = -1.5\Delta_{\text{green}}$. Thus we obtain $\Delta_{\text{green}} = +0.92$ gs, and $\Delta_{\text{red}} = -1.4$ gs. Therefore, in calibrations in $\lambda 5250$ and $\lambda 6103$, 1.71 and 3.28 gs/mm respectively, we obtain $\Delta_{\text{red}} = +0.5$ and $\Delta_{\text{green}} = -0.43$ mm. These corrections were used in calculating the flux differences $F_S - F_N$ (#3).

Let us point out some other peculiarities of the recordings. 1) The slits of the magnetograph photometer, as customary, were placed at the steepest part of the line contour: for $\lambda 5250$ in order V the slit was 1.8×0.7 mm (which corresponds to a distance $\Delta\lambda = 0.064 \text{ \AA}$ from the slit to the center of the line), and for $\lambda 6102.7$, 2.0×0.7 mm,

which corresponds to $\Delta\lambda = 0.08 \text{ \AA}$). 2) In most cases, the solar image at the slit of the spectrograph equalled 200 mm, so a slit 60 X 1.0 mm corresponds to a square 2.5" wide and 9" high. A slit 60 X 1.5 mm is only used when (winter and spring) the solar image is 350 mm, which corresponds to the exact resolving power 2.5" X 9" (Table 1). 3) All the recordings were made taking into account the possibility of a quiet sun, where no expressed activity centers on the disk are registered on the spectroheliograms. The occasional absence of visible details on the disk compelled us to use a solar image reduced to 31 cm for guiding and scanning where scanning was carried out along the western limb. #4) Until issue of the double magnetograph 10 August, 1966, calibration of recordings in $\lambda 5250$ was done as usual, by registering prominences on the E and W limbs of the sun (1.5' from the limb) with the aid of a $+\frac{1}{2} \lambda$ -plate attachment to the polaroid as per the formula [6]

$$(E - W) = 1600 \text{ gs.} \quad (1.1)$$

After 10 August, 1966, recordings in $\lambda 5250$ were made with a brightness compensator, in which case, instead of equation (1.1) we have

$$2,75 \frac{I_e}{I_0} (E - W) = 800 \text{ gs,}$$

of where I_e/I_0 -- the darkening in that part of the disk being recorded. For the polar zones chosen by us, $I_e/I_0 \approx 0.55$, and calibration was determined from the condition

$$1,5(E - W) = 800 \text{ gs.} \quad (1.2)$$

Recording 13 March, 1966, was carried out with a brightness compensator (for its calibration (1.1)). Registrations in $\lambda 6102.7$ and H_{α} are

always made with a brightness compensator. For the line H_{α} the Landau factor $g = 1.14$ is 2.6 times less than for $\lambda 5250$. Therefore, considering that the wave length ratio of H_{α} and $\lambda 5250$ is 1.25, we obtain, instead of 1600 gs, the value $1600 \cdot \frac{2.60}{1.25} = 3400$ gs, so that for H_{α} , the equation for calibrating with a brightness compensator is [6]

$$(E - W) = 3400 \text{ gs} \quad (1.3)$$

on condition that calibration is carried out with a $\frac{1}{2} \lambda$ plate especially for the wave $\lambda 6563$. If it is carried out with a $\frac{1}{2} \lambda$ plate for $\lambda 5250$, then $E - W$ must be multiplied by still another value which, according to our measurements, is 1.55. Analogously for $\lambda 6102.7$, $g = 2.0$, and the value $E - W$ with brightness compensator:

$$E - W = \frac{1,14 \cdot 6,56}{2,00 \cdot 6,40} \cdot 3400 = 2070 \text{ gs.} \quad (1.4)$$

Exactly as before, if calibration is carried out with the usual $\frac{1}{2} \lambda$ -plate (for $\lambda 5250$), the factor for $E - W$ is 1.35, according to our measurements.

2. The Effect of Resolving Power

It was found in [1] that, when scanning the same region at different resolving powers (from 27" to 4.5"), maximum field strength in magnetic "elements" increase by 2 - 3 times at most (Fig. 3, [1]). This was done for one certain section which contained only 3 elements. In order to clarify the effect of resolving power on the statistical results of general field measurements, based on averaging data on many elements, it would be necessary to scan larger areas at different

resolving powers, which was done in the summer of 1965 and was used [7] to clarify the question of concentration of the field in thin filaments. Successive recordings of a 120" X 120" section at resolutions $R = 27''$ (slit height, 3 mm, Series I)¹, $R = 9''$ (height 1 mm, Series II), $R = 4.5''$ (height 0.5 mm, Series III) and $R = 2.25''$ (height 0.25 mm, Series IV) were made so that the same section was scanned at different R's, allowing a comparison of statistical results at different R's. A detailed description of the material is given in [7]. We reworked this material for the express purpose of determining the effect of resolution on our systematic measurements of the general field. Analysis lead us to consider a number of elements in the field within given limits: 0 - 2, 2 - 4, 4 - 6 gs, etc., for the entire 120" X 120" region, recorded at a given resolution. Since (#3) there are S-polarity components, the N- and S-poles were analyzed separatel6. Records made on July 13, 18, 21, 22 and 23 were used for the N-pole, and for the S-pole, only three records from July 24, 25 and 26, 1965. Distributions (histograms) of a number of S- and N-polarity components at both poles at different resolutions are given in Table 3, from whence it follows that the average field strength of a given polarity

$$\bar{h}_{S,N} = \sum h_i v_i,$$

where v_i --frequency of occurrence (percentage of the general number of cases) of the field strength h_i , increases with resolving power R (Fig. 2,a) which might be expected to agree with our data given in [1] Fig. 3.

¹Actually the barrel was screwed to 2 mm = 18".

Our measurements show maximum average field strength increase to 30% as resolution is increased from 27" to 2.25", while in [7], we found a sharper increase to \sim 60%.

Rather unexpected is the considerable increase (1.5 - 2.0 times) in net mean field strength, $\bar{h}_S - \bar{h}_N$ at the S-pole and the small increase in $\bar{h}_S - \bar{h}_N$ at the N-pole (crosses in Fig. 2,a). (Measurements in [7] indicate a twofold increase in this value.) Of course the increase in \bar{h}_S , \bar{h}_N and the difference $\bar{h}_S - \bar{h}_N$ are not evidence of an average increase in \bar{H} for the entire section recorded, and cannot vary with resolution (see below) because the recordings mentioned embraced, not the whole section, but only certain parts which were the same for different R (see scanning procedure at various resolutions in Fig. 3).

Let us review the problem of average field value more carefully at various apertures. Assume that the field consists of tiny "elements" of a purely longitudinal + and - pole with a Π -shaped distribution inside element so that the field outside the elements equals zero. We will assume that the brightness and the spaces between them are equal. The field strength, measured with magnetograph slit aperture area S, will be in general

$$\bar{H} = \frac{1}{S} \int H ds = \frac{1}{S} (\sum H_+^+ S_+^+ + \sum H_-^- S_-^-) = \frac{1}{S} (\bar{H}_+ S_+ + \bar{H}_- S_-), \quad (2.1)$$

where integration is carried out over the whole area S; H_+ , H_- -- average strengths for elements of + and - polarity; S_+ , S_- -- measured areas of + and - elements, respectively; it is obvious that $S_+ + S_- \ll S$.

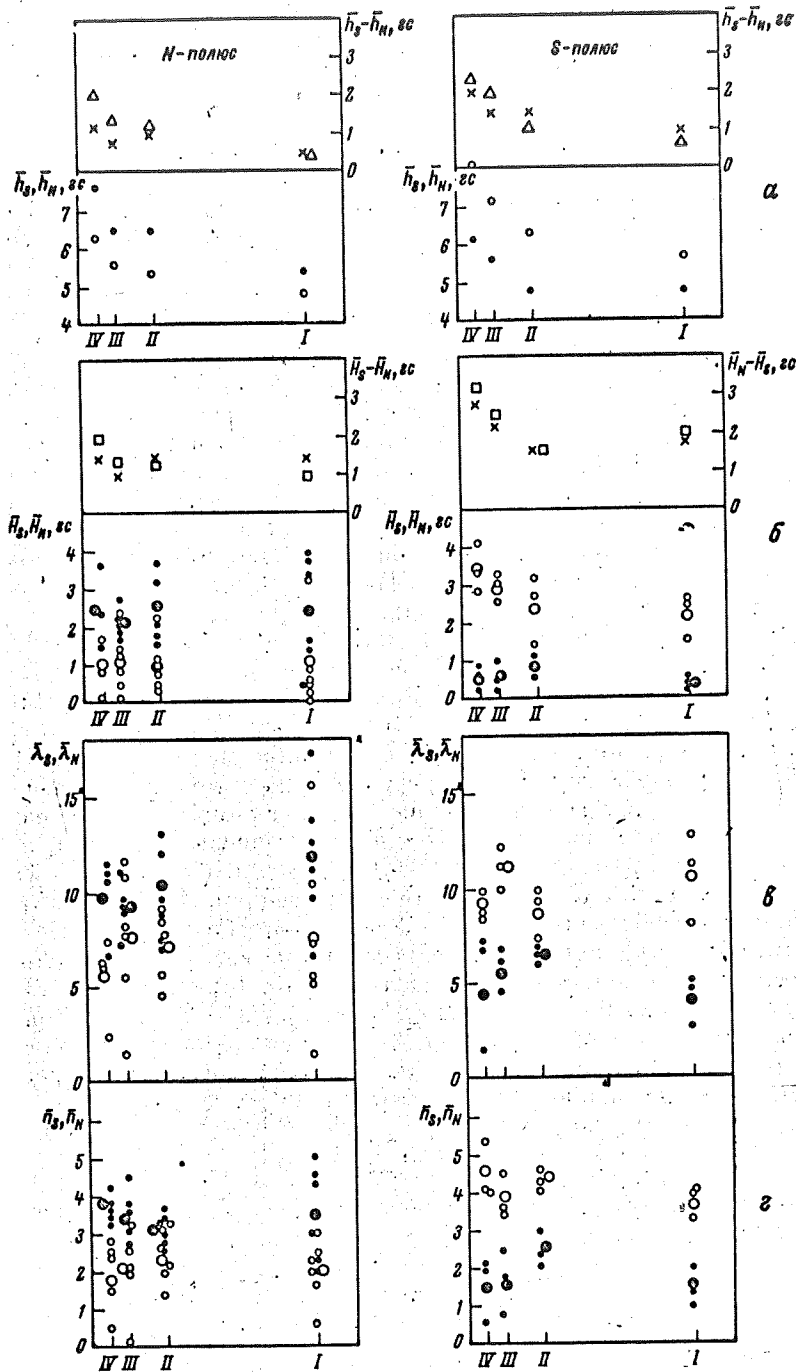


Fig. 2: Variations in characteristic polar field magnitudes at various resolutions: I = 27"; II = 9"; III = 4.5"; IV = 2.25". a--mean (weighted) intensity; б--mean flux intensity; в--mean length; г--mean number of field components. The large dark and light circles are the mean values for several days (see text), and the triangles were obtained from [1].

Table 3. Histograms of Field Strength at Various Resolving Powers

Напряженность, ес Pressure, gs	Серия Series							
	I		II		III		IV	
	S	N	S	N	S	N	S	N
N-полюс N-pole								
0-2	5	2	2	3	5	4	2	2
2-4	26	22	26	37	39	48	30	12
4-6	24	17	44	41	66	43	53	33
6-8	13	8	21	22	41	30	34	34
8-10	2	3	18	6	22	17	33	17
10-12	5	3	5	3	16	1	14	6
12-14	4	—	4	4	4	4	18	—
14-16	1	—	1	1	6	3	10	5
16-18	—	—	3	—	2	1	2	2
18-20	—	—	1	—	1	—	3	—
Среднее, ес. . .	5,40	4,90	6,49	5,34	6,44	5,61	7,62	6,42
S-полюс S-pole								
0-2	2	1	5	1	2	—	—	1
2-4	11	21	16	25	10	12	11	12
4-6	14	35	10	22	24	26	21	34
6-8	5	17	—	12	13	27	14	39
8-10	1	7	5	9	7	29	—	18
10-12	1	5	1	6	—	19	3	21
12-14	—	1	1	1	1	6	4	12
14-16	—	—	1	2	—	3	—	5
16-18	—	1	—	1	—	—	—	4
18-20	—	—	—	—	—	4	—	1
Среднее, ес. . .	4,74	5,74	4,78	6,33	5,61	8,13	6,08	8,11

Let us review the simple case where our elements have the same strength

$\bar{H}_+ = -\bar{H}_- = H$, the same shape (square) and area (equal to 1); then,

$$\bar{H} = \frac{1}{S} (S_+ - S_-) \quad (2.2)$$

and let us review the case given in Fig. 4, when a given section, containing four elements (three with +H and one with -H distributed as shown in Fig. 4), is first scanned with a slit that encompasses the entire section (enclosed in dash-line)--Case I; then 3 times in succession with a slit 3 times smaller (Case II); and finally with a slit 6 times smaller, successively 6 times (Case III), where the slit

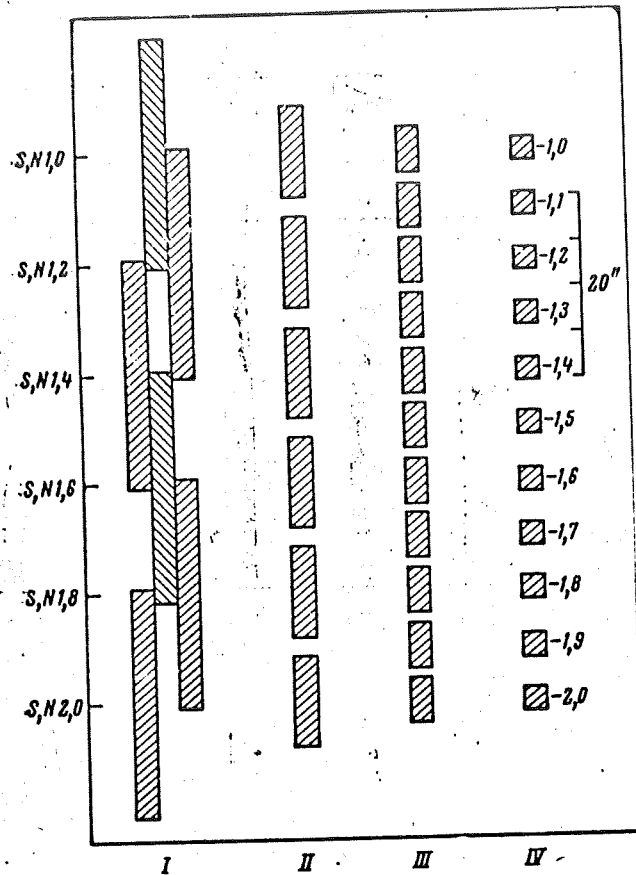


Fig. 3: Distribution and size of slits during consecutive scanning of the same section (S, N_{1.0} - S, N_{2.0}) at different resolutions (Roman numerals).

width is considered constant and equal to the width of a section whose area is taken as 18 units. Then we have, corresponding to the various cases, the following results:

Case I

$$S_+ = 3, S_- = 1$$

$$\bar{H} = \frac{H}{18}(3-1) = \frac{1}{9} H$$

Case II

1st section: $S_+ = 0, S_- = 0, \bar{H}_1 = 0$
 2nd section: $S_+ = 1, S_- = 1, \bar{H}_2 = 0$
 3rd section: $S_+ = 2, S_- = 0, \bar{H}_3 = \frac{2}{6} H$

Average field strength:

$$\bar{H} = \frac{1}{3}(H_1 + H_2 + H_3) = \frac{1}{9} H$$

Case III

- 1st section: $s_+ = 0, s_- = 0, \bar{H}_1 = 0$
- 2nd section: $s_+ = 0, s_- = 0, \bar{H}_2 = 0$
- 3rd section: $s_+ = 1, s_- = 1, \bar{H}_3 = 0$
- 4th section: $s_+ = 0, s_- = 1, \bar{H}_4 = 0$
- 5th section: $s_+ = 2, s_- = 0, \bar{H}_5 = \frac{2}{3}H$
- 6th section: $s_+ = 0, s_- = 0, \bar{H}_6 = 0$

Average field strength:

$$\bar{H} = \frac{1}{6} \left(\frac{2}{3}H \right) = \frac{1}{9}H.$$

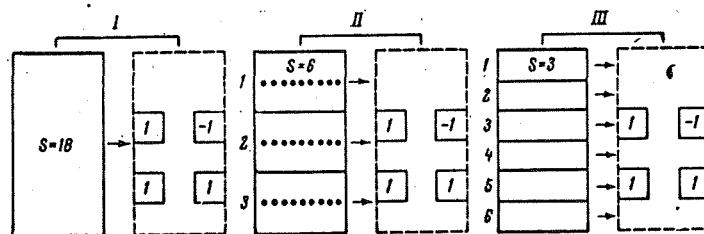


Fig. 4: Scanning the same section (dash-line), which contains 4 field components (small squares), using apertures of different sizes (case I, II, and III--see text).

Thus, upon scanning a given region at different resolutions so that the entire region is covered uniformly, without omissions and overlaps, the average field cannot vary, which is correctly shown in [8].

In other words, net magnetic flux does not depend on the resolving power if the same region is covered at various resolutions. But,

recording at resolution II (Fig. 4), the section is scanned only twice (Fig. 4, dotted line), then for the first section we obtain

$$\bar{H}_1 = 0; \text{ for the second, } \bar{H}_2 = 2/6H \text{ and the average field } \bar{H} = (0 + 1/3H)/2 = 1/6H \text{ greater than the field at low resolution. If analogously,}$$

with slit III, we scan only sections 3, 4 and 5, then we obtain an average field of $\bar{H} = 1/3 \cdot 2/3H = 2/9H$, which is still greater than at resolution II. Hence, we obtain a twofold increase in the average field due to incomplete scanning of the region. Apparently, this effect showed up in [7], where an average net flux increase was discovered, which is physically impossible. From the scanning diagrams in Fig. 3, it is apparent that the average field for Series IV will be considerably increased (possibly twofold as in the cited example); and for Series I, decreased, which may give the increase mentioned.

Therefore, all of the recordings were revised to eliminate the over estimation in Series I (only the numbers are shown in Fig. 3), taking into account that Series IV recordings could hardly be compared with the others without being reduced by some factor. Those values proportional to N- and S-polarity field fluxes were determined: namely, the areas bounded by the recorded field and the zero line, i.e. the values

$$F_{S,N} = \int H_{\parallel} dl \quad (2.3)$$

taken separately for S and N fluctuations. The sum of these areas for a given section, dividing it by the length L, gives the average field of given polarity $F_{S,N}/L$; then the average of all sections outside the given area is calculated as $\frac{1}{n} \sum F_{S,N}/L$, where n--the number of sections. By an analogous method, the mean length of S- and N-polarity elements $\bar{\lambda} = \frac{1}{n} \sum \lambda_{S,N}$ and the average number of elements were found. The results of all different measurements for all data cited above are

given in Fig. 2, a, b and c individually for the N-and S-poles (see also Table 4). At the N-pole, where the average is well established by measurements, if the values \bar{H}_S and \bar{H}_N increase at all, it is negligible, which underscores the stated fact that deflection amplitude increases with resolution. However, no increase in $H_S - H_N$ with resolution (Fig. 2, graph, top) was detected in relationship with the above statement of net flux constancy (even if one considers that the value of this difference for Series IV must be reduced by a factor of ~ 2). An increase in field strength with resolution is compensated by reducing the size of the field elements. As for the S-pole, which is established by only three measurements, an increase in net field $\bar{H}_N - \bar{H}_S$ with resolution (in accordance with an analogous field increase $\bar{h} = \bar{h}_N - \bar{h}_S$ in fig. 2,a) is observed along with increases in H_N and H_S .

An increase in average field with resolution, at a given polarity, is apparently related to the fact that the mutual annihilation effect of fields within the limits of slit range decreases with aperture (for example, in Series I, Fig. 4, the + field was $1/9H$, but for a slit 3 times smaller, it was $(\frac{1}{6}H + \frac{2}{6}H)\frac{1}{3} = \frac{1}{6}H$). However, an increase in net field, $H_N - H_S$ for the S-pole is at best, fictitious, and in essence, reflects only an increase in the field H_N , since the mean field strength H_S (Table 4) on the average is only 0.6 gs, which is considerably below mean total noise amplitude, as is shown by its dependency on slit height in Fig. 5. In general, noise may strongly affect the measurements in Series IV, although common field fluctuations

Table 4

Серия Series	F_S, gs	F_N, gs	$F_S - F_N, \text{gs}$	λ_S	λ_N	n_S	n_N
N-полюс N-pole							
I	2,36	0,92	1,49	11,8	7,59	3,51	1,98
II	2,47	1,01	1,46	10,1	7,11	3,13	2,49
III	2,06	1,06	1,00	9,18	7,58	3,52	2,09
IV	(2,64)	(0,86)	(1,78)	(9,90)	(5,55)	(3,78)	(1,80)
S-полюс S-pole							
I	0,37	2,17	-1,80	4,26	10,6	1,43	3,76
II	0,84	2,38	-1,54	6,60	8,80	2,53	4,33
III	0,62	2,91	-2,29	5,90	11,1	1,70	3,86
IV	(0,60)	(3,40)	(-2,80)	5,26	9,13	1,60	4,53

are well separated, owing to their systematic character. Indirect analysis of S-pole recordings for 24, 25 and 26 July, 1965, shows an almost complete absence of S-polarity fluctuations, but the majority of fluctuations studied were simple, long "period" noises; while at the same time, strong (up to 35 gs) N-polarity fields were noticed. This is also illustrated on an isogauss field map drawn for one of these days (Fig. 6). Let us now review how the volume of information on the general solar magnetic field varies with resolving power--to be exact--when transferring from our most frequently used resolving power (2.5" X 9") to the resolution used, for example, at Mount Wilson Observatory: R = 23" X 23". Information loss at greater aperture would not exist if there were no noises--all of the small elements would add their part to the mean field

$$\bar{H} = \frac{1}{S_0} \sum H_i s_i$$

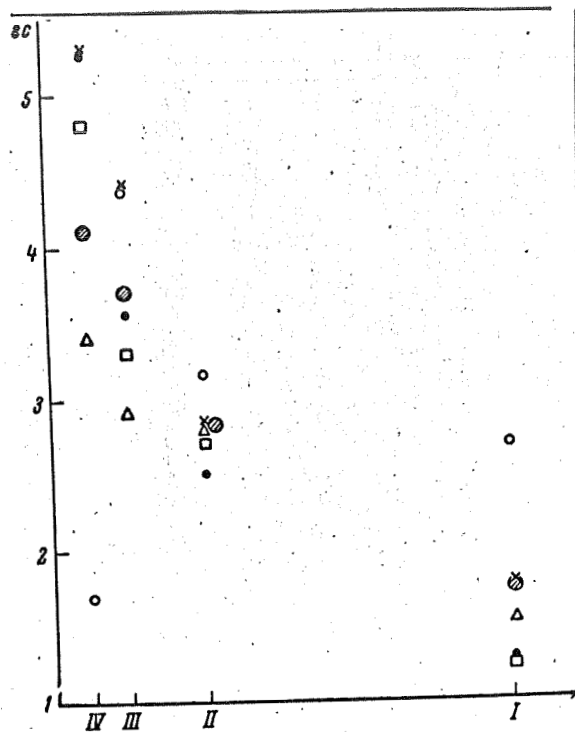


Fig. 5: Dependency of mean (total) noise amplitude on resolution for different days. The large striped circles are mean values.

where S_0 is the aperture area, and recording at low resolution would only differ from high resolution in that the former would be an average of the latter. However, due to the presence of noise, a small element with area $s_i \ll S_0$ at low resolution gives only a very weak field

$H = \frac{s_i}{S_0} H_i$ (even at considerable H_i), which may fall below the sensitivity threshold of the magnetograph, i.e., the field signal compared with the noise. Our problem is to find which field element dimensions and field strengths mark the onset of information loss. Mean noise level (based on many measurements) for the Crimean magnetograph [1] is

$$\bar{h} = 2,03 \text{ gS}$$

(for a specially chosen photoelectric multiplier EMI); this we took as the threshold signal. The signal magnitude varies as the square

root of the light flux into the spectrograph, i.e. the square root of the entrance aperture (slit) area at the same d/f. Thus, our threshold signal for a 23" X 23" slit will be

$$\bar{h}' = 2,0 \sqrt{\frac{9'' \times 2'',5}{23'' \times 23''}} = 0,42 \text{ gs.} \quad (2.4)$$

For us, d/f of the intake optics equalled 1/50; but at d/f = 1/150 (Mount Wilson), the mean threshold noise would in no way be less than 1 gs at the same time constant $\tau = 2.5^s$. Even taking it at 0.5 gs, all of the field elements, for which H_M and area s satisfy the inequality¹

$$H_M \frac{s}{S_0} \leq 0,5 \text{ ec,} \quad (2.5)$$

give a signal \leq noise threshold, using a 23" X 23" slit.

At the same time, for a slit $S_0 = 2.5'' \times 9''$ and analogous inequality is

$$H_C \frac{s}{S_0} \leq 2 \text{ ec.} \quad (2.6)$$

Fig. 7 gives the dependency of maximum H_M and H_C on s/S_0 -curves I and II show that all elements with fields and dimensions below curves I and II lie within the noise limits. The weight mean strength of general field elements is in agreement with [1] and that given in this work may be taken as 5 gs. It follows from Fig. 7 that at a 23" X 23" resolution and strength of 5 gs, only those elements will be registered whose dimensions are

$$d \geq d_2 = 7'',5, \quad (2.7)$$

¹Reference [2] gives the mean square noise equal to 0.1 gs, at a slit height of 70" and time constant of 5^s; upon rechecking on a 23" X 23" slit (at a width of the initial slit of 2"), we obtain a noise of 0.2 gs, but at a time constant of 2.5^s it would be ~ 0.3 gs. In [9], for a 10" X 10" slit, the noise is ≤ 0.5 gs at $\tau = 5^s$, which gives a threshold noise, at $R = 23'' \times 23''$ and $h' \leq 0.5/2.3 = 0.2$ gs, or 0.3 gs at $\tau = 2.5^s$. If we consider that the calibration in ref. [2] and [9] are lower by a factor of 2 in comparison with ours, then the threshold signal will be 0.6 gs in relationship to the value of 0.5 gs chosen by us.

i.e., greater than the radius of correlation [5]; whereas, at a resolution of 2.5" X 9", elements with the same strength and with dimensions $> 3''$, or even higher, are registered if it is considered that the slit is 2.5" in width. According to the data in [5] (Table 10, Fig. 20), this indicates that no less than 30% of all elements are lost at a 23" X 23" resolution, while we lost no more than 10% of all elements. Fig. 8 shows a comparison of maps of our data and Mount Wilson Observatory data (footnote on pg.) for 2 August, 1965; from this, it is apparent that our map shows 158 elements, i.e., we have 1.72 times more detail (in number) than the Mount Wilson map, regardless of a "gap" of about 2 in our recordings at the pole and similarly, for a disk of ~ 4 (ratio of the distance between successive sections and the top of the slit). The gap in the Mount Wilson recordings equalled 1, the disk was uniformly covered by the recordings.

Up to this time, we have considered differences in the time constant τ . The Mount Wilson map in Fig. 8 was obtained in 80^m, which corresponds to a scanning rate of 23"/sec. Since the speed R/τ does not cause serious information loss, then $\tau \approx 1^s$, while for us $\tau = 2.5^s$. This increases the threshold hold field (2.5) by a factor of $\sqrt{2.5}$, i.e. it gives 0.79 gs instead of 0.5 (noise drops as the square root of $1/\tau$), which means that only elements with $d > 10''$ are registered, which is no more than 50%. If we take $\tau = 2.5^s$ at a speed of 23"/sec, we obtain an amplitude drop in the ratio $(1 - e^{-2.5})/(1 - e^{-1})$ for all signals, i.e., by a factor of 1.4; according to curve I, Fig. 7, this leads to information loss for all

elements when $d > d_2 = 8.5''$, which is about 45%.

Besides this, it should be considered that, at the poles, there is an uncompensated decrease insensitivity by a factor of 1.2 - 2.0 due to a brightness drop at the limb of the disk, which leads to an increase in threshold (2.5) to 1 gs at most, and to loss of elements with $d > 12''$. Thus, the method of registration used at Mount Wilson Observatory leads to loss of information for no less than 50% of the elements¹ of the general magnetic field, but has the advantage of covering the entire field uniformly. We lost only 10% of the information, but the disk was covered only half as thoroughly as it should have been, based on data on the radius of autocorrelation (7.5''): the interval between sections should not be more than double the radius of autocorrelation; otherwise, new field elements appear. Our recordings are usually carried out with a 25'' interval; and even at a speed of 2''/sec (which is twice greater than R/τ), recording the disk with this type of gap takes at least 8^h. All the same, in understanding the physical nature of the general field, to record at high resolution, even if not the whole disk, is more preferable than recording a larger section that contains a known area of chaoticity in field distribution (outside of the active zones)--this follows from the recordings of the field over the entire disk and

¹The loss of $\sim 50\%$ of the information in recording with a 23" X 23" slit may immediately be confirmed by histograms of average field strength (Fig. 10) which show that field elements with $H_n > 6$ gs (according to the Mount Wilson calibration, ≥ 3 gs--the magnitude at which isogauss on the maps of this observatory begin) constitute no more than 50%.

from net field distributions with magnitude as given below (Figs. 13 and 14).

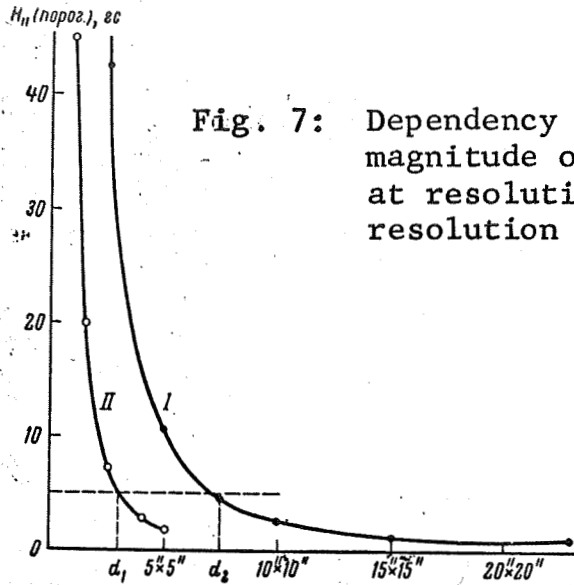


Fig. 7: Dependency of threshold signal on the magnitude of magnetic field components at resolution $23'' \times 23''$ (curve I) and resolution $2.5'' \times 9''$ (Curve II).

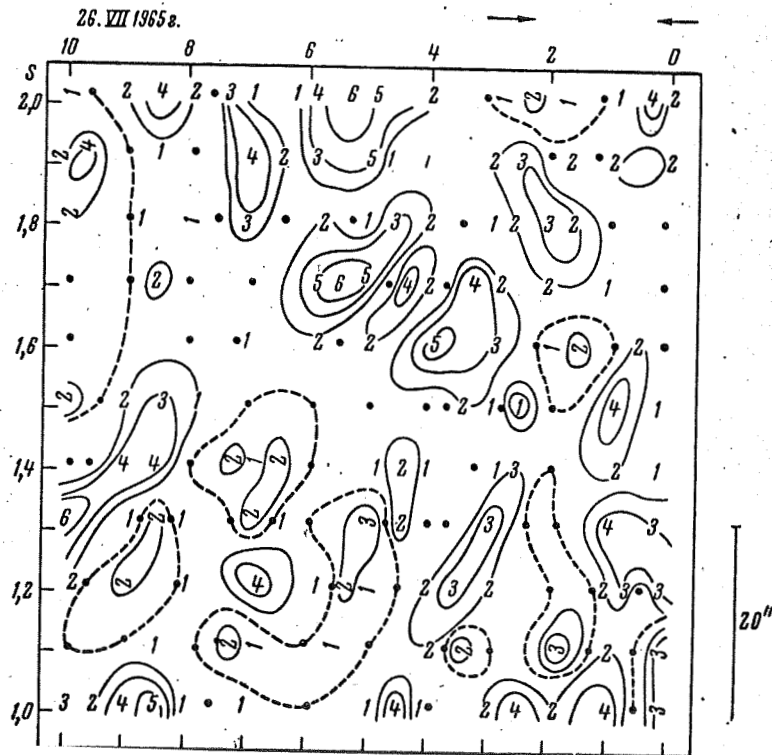


Fig. 6: Map of the field 26 July, 1965, obtained at resolution $R = 4.5''$: calibration, $1 = 2.35$ gs; vertical numbers are N-polarity, horizontal numbers are S-polarity.

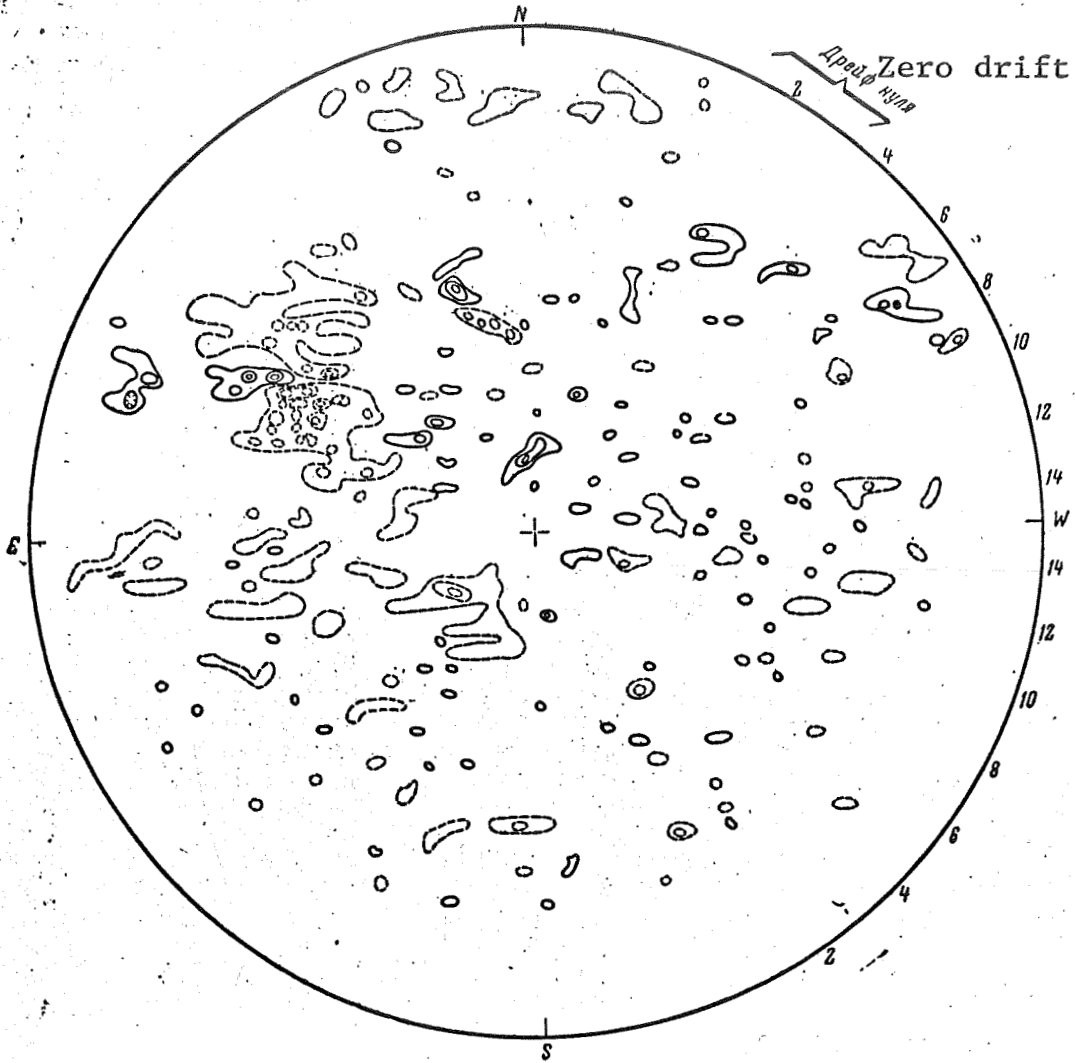


Fig. 8 : Comparison of general field maps of the entire disk for 2 August, 1965, obtained at Mount Wilson Observatory (left) and in Crimea (right): Isogauss begin at 3 gs: N-polarity, solid line; S-polarity, dashed line; the numbers at the right are the numbers of the sections made in the Crimean.
See next page.

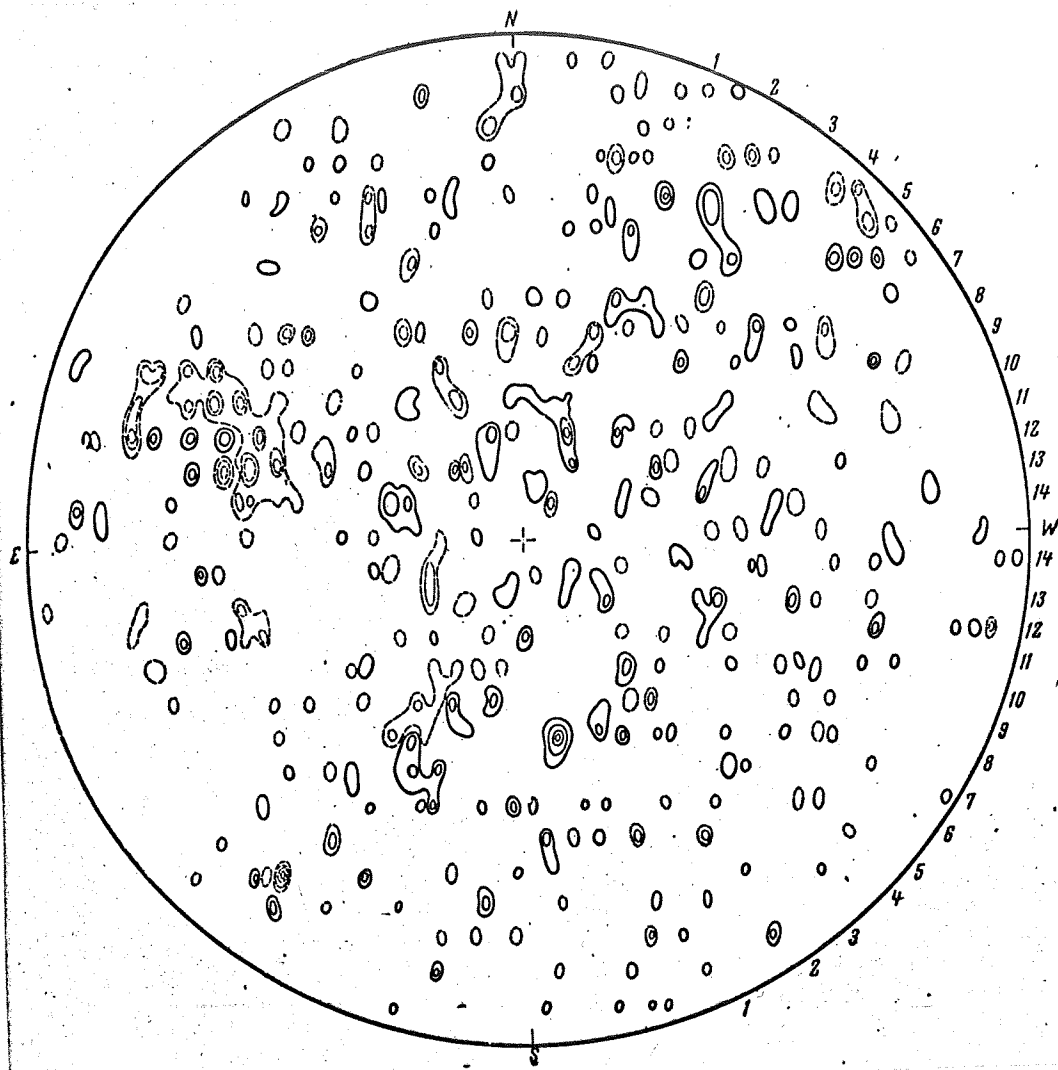


Fig. 8,a

3. The Polar Field and Its Variations

As in [1], frequency distribution histograms were constructed for the occurrence of maxima in fluctuation amplitudes of S- and N-polarity fields at intervals of 0 - 2, 2 - 4, 4 - 6 (etc.) gauss on each day of observation for the entire zone near the pole, shown in Table 1. Using these histograms, we found the weighted mean field strength value

$$\bar{H} = \sum H_{i,v}(i)$$

For the given polarities H_S and H_N , for each day of observation. Histograms were not made for separate days, but the values H_S and H_N for the N- and S-poles are given separately in Fig. 9 and in Table 6. On those days when we recorded the whole disk, the recordings were divided into 2 zones: the polar (sections 1 - 8, from ~ 30 to $\sim 70^\circ$ latitude) and the equatorial (sections 9 - 14 from 0 to $\sim 30^\circ$); for both zones the values \bar{H}_S and \bar{H}_N were determined: the equatorial values have been especially set apart in Fig. 9. This value distribution immediately shows a predominance of S-polarity at the N-pole, and N-polarity at the S-pole in the majority of cases. A remarkable rise in the strength of both polarities toward middle year, and a drop toward year end, are noted. It should be remembered that each value in Fig. 9 is a weighted average over 50 - 80 (on the average) elements of a S- or N-polarity field.

Examination of the histograms does not allow, as in 1964, allocation of all the data to a certain characteristic period.

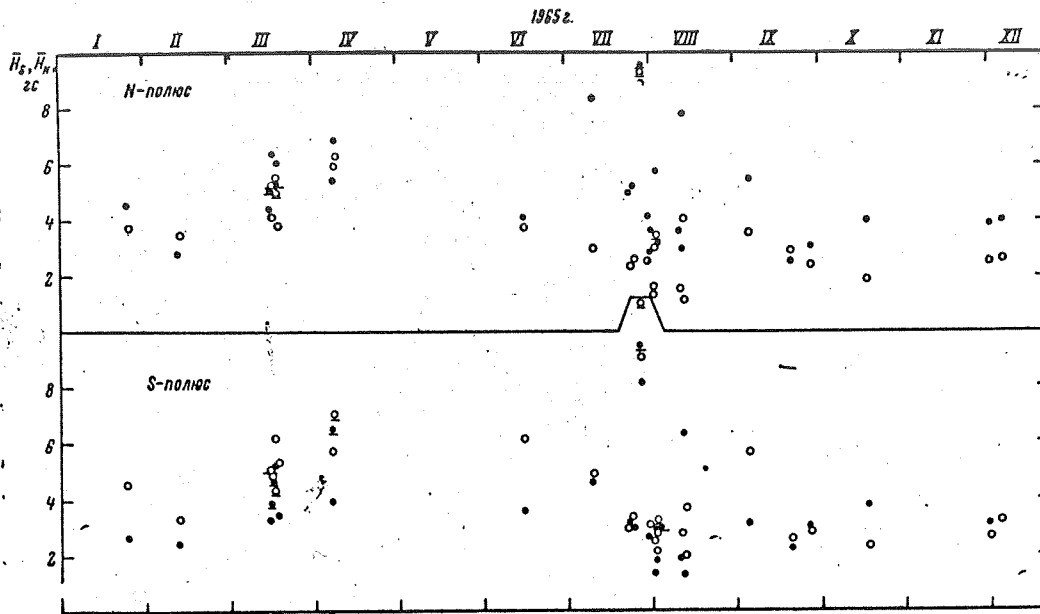


Fig. 9: Mean (weighted) field strength for N- and S-polar regions as a whole on different days of 1965: dots, S-polarity; circles, N-polarity.

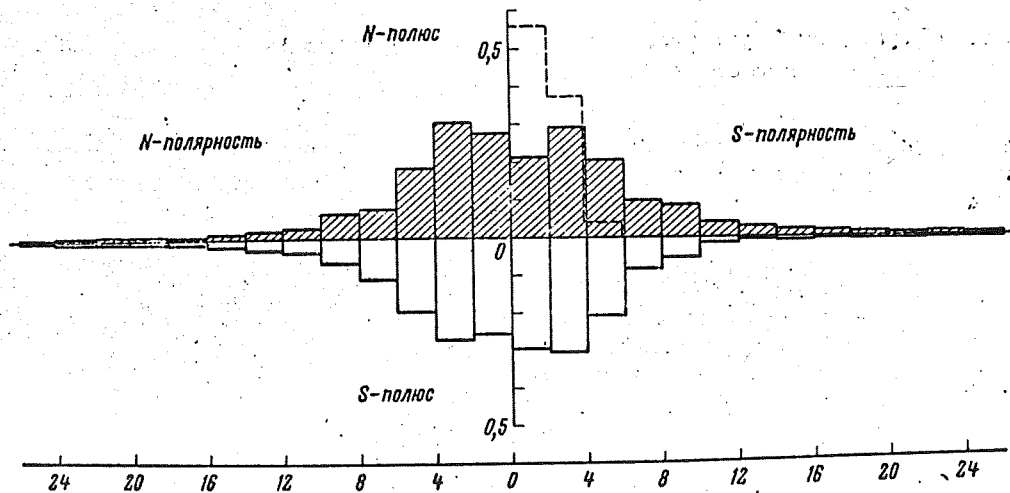


Fig. 10: Average histograms, for 1965, of the frequency of field components of different polarity and strength for the N (stipped columns) pole and the S-pole: the dashed line is the noise histogram per [1].

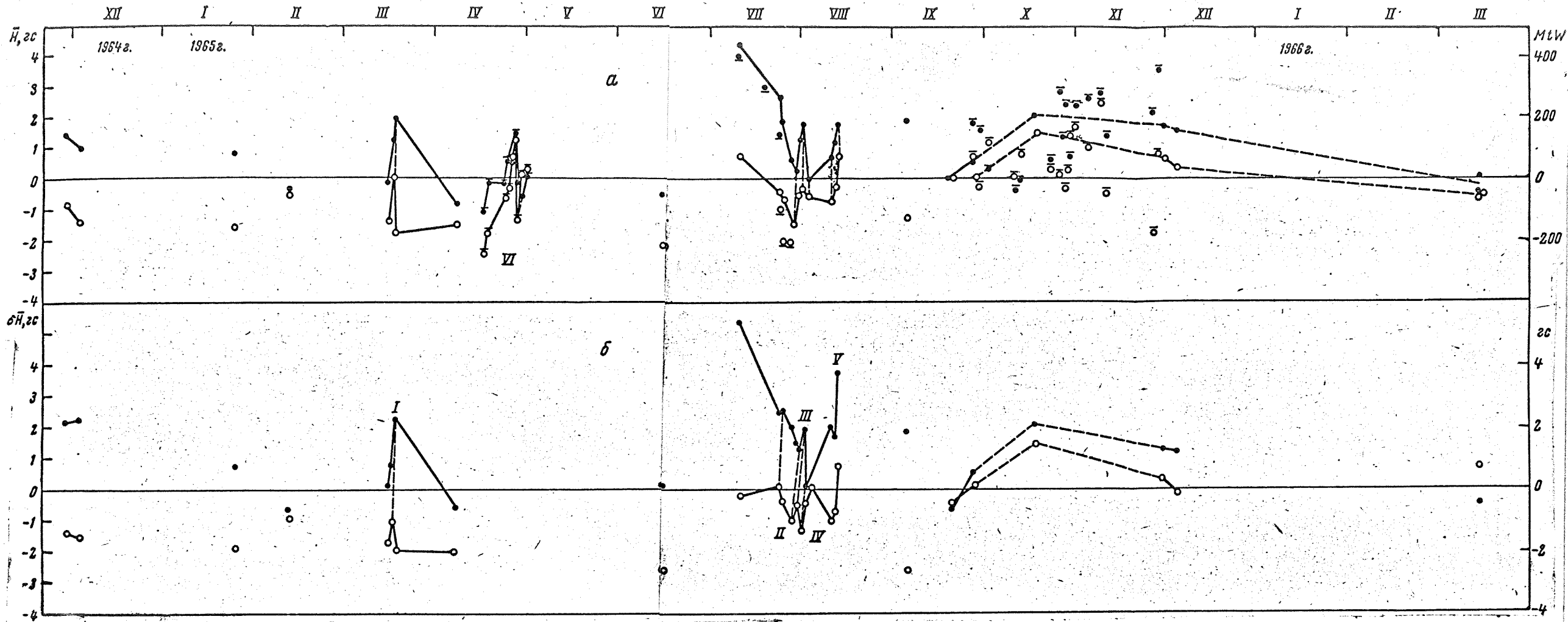


Fig. 11: Net field strength \bar{H} (as per flux magnitude, a and \bar{H}^1 (as per weighted mean value), on different days: dots, N-pole; circles, S-pole. Points and circles with the dash below are the same as [7]; those with dashes above are Mount Wilson data. I, II, etc. indicate peaks of rapid fluctuation which exhibit a delay at the N-Pole. The unit of the Mount Wilson scale equals $2 \cdot 10^{18} \text{ mx} \cdot \text{v}$.

Table 5: Histogram of Field-Occurrence Frequency, 1965

$H_{ }, \text{gc}$	Polarity			
	N-полюс		S-полюс	
	S	N	S	N
0-2	415	446	519	514
2-4	537	497	531	545
4-6	394	304	363	392
6-8	190	128	148	222
8-10	162	103	97	132
10-12	74	48	31	66
12-14	55	40	13	60
14-16	32	21	16	36
16-18	21	7	8	15
18-20	18	12	6	11
20-22	11	16	2	5
22-24	15	7	1	5
24-26	8	3	5	6
Σ	1962	1635	1740	2009
\overline{H}, gc	5,28	4,65	4,04	4,83

Table 5 summarizes the frequency of field occurrence, H_S and H_N , for the entire year, 1965, and fig. 10 is a summary histogram for 1965. It does not show the type of distributional asymmetry at the N-pole, as in 1964: the values are often found to be more or less the same at both the N- and S-poles, and equally so for S- and N-polarities. Noteworthy is the appearance of a small number of high intensity fields (up to 20 - 25 gs, without correcting for resolution) in the polar zones, especially among S-polarity fields at the N-pole.

The minimum at 0 - 2 gs is attributed to the fact that the majority of such fluctuations are noises (the noise histogram is indicated by the dashed line).

Table 5 shows that most S-polarity fields were at the N-pole (5.3 gs); they are almost equalled (in terms of average weight) by the 4.8 gs N-polarity field at the S-pole. The average net field at the N-pole was +0.6 gs (S-polarity); and at the S-pole, 0.8 gs

(N-polarity); hence, the total average for 1965 is approximate. The sun may assimilate a dipole, as in 1964, when the field at the S-pole was totally nonexistent for the first half year.

However, there were periods when the behavior of the general field was in sharp contrast to a field characteristic of a dipole. In due course, the behavior of the field is characterized by the quantity

$$\delta H = \bar{H}_S - \bar{H}_N, \quad (3.1)$$

found in fig. 11,b; for thoroughness, we have added here, the last 2 months of 1964 and observations for 13 March, 1966. Along with these values, the average values of the quantity

$$\bar{H} = \frac{1}{L} (F_S - F_N) = \frac{\Delta F}{L}, \quad (3.2)$$

where F_S and F_N -- total fluxes of S- or N-polarity fields for a given section of length L ,

$$F_{S,N} = \int H_{\parallel} dl. \quad (3.3)$$

The quantity F , as in [1] was calculated by planimetry of an area bounded by the recording and the zero line in an area of S- or N-deflection and expressed in gs-mm of recording length; since the cost of 1 mm of recording in seconds of arc is known, the quantity F can easily be expressed in mksv (see below)

Table 6 gives average values of $F_S - F_N$ (in units of gs/sec arc), and F_S/F_N is characterized by a predominance of flux of one polarity over the other. Mean \bar{H} (3.2) was obtained by averaging the ratio $\Delta F/L$ for each section; this is better than averaging ΔF and L individually and then their ratio, because the length L varies little.

The variation in \bar{H} with time is shown in fig. 11a. Comparison of F_S/F_N in table 6 with the mean values of λ_S/λ_N (length ratio of N and S elements), and also the mean ratio of the number of elements (n_S/n_N), demonstrate the rather obvious proportionality between F_S/F_N and these numbers (graphs not plotted), since the average of the quantities, themselves, is $\bar{F} = \overline{Hn\lambda}$ [1]. It is also apparent that the lengths of the elements, and not their intensity and number, have the greatest effect on the magnitude of F .

Fig. 11b shows similar behavior for δH , the net field based on the frequency distribution of maximum amplitudes, and H , the net field based on fluxes, although, some points of difference are that they occur due to "admixtures" of protracted elements of a weak field or small elements of a strong field. As far as each point is concerned and these are averages of 60 - 80 measurements - these fluctuations, even the rapid ones, are completely valid. These rapid fluctuations are on the order of 24 hours, e.g., 15 - 17 March, 24 July - 2 August and 10 - 12 August, and recur just as well at both S- and N-polarities, in which case, the peaks, especially the minima, at the N-pole are repeated at the S-pole after a lapse of 1 - 2 days, for the cases cited. For example, in March the field at the S-pole reached a maximum on the 16th and dropped to normal on the 17th; and at the N-pole, it reached a maximum only on the 17th; similar effects were observed in July. The following picture is obtained:

Pole	I	II	III	IV
	max $H, \delta H$	max δH	min $H, \delta H$	max δH
S	16.III	23.VII	27.VII	29.VII
N	17.III	24.VII	29-30.VII	1.VIII

It shows in 4 cases, a lapse of 1 - 2 days for peak magnitude of δH or \bar{H} in the field at the N-pole in comparison with the S-pole. If these lapses are due to a magnetic disturbance propagated from the S- to N-polar region, then its velocity would be ~ 5 km/sec, which approximates turbulence velocity in the upper layers of the solar atmosphere.

Let us review this effect critically. If it were related to zero error, the occurrence of peaks would be simultaneous: all values at both the N- and S-poles for a given day would be more or less equally shifted (with respect to N- or S-polarity). And moreover, analysis of the recordings would show no basis for attributing this effect to zero error in the given cases. Calibration errors, which would increase or decrease N- and S-field intensity values, would obviously increase the difference $H_S - H_N$, the net field \bar{H} (or δH), by the same factor. First of all, however, this error, like zero error, appears equally and simultaneously in the field at both N and S-poles; and secondly, it does not exceed, as a rule, 30%, whereas we are dealing with variations 2 - 3 times greater and more (a 30% error is inevitable due to $\sim 5^m$ periodic pulsations in velocities on the Sun).

Due to rotation, a 240" section registered over α would be almost

Table 6: Data on the Polar Field and Its Variations

№ п/п	Дата	$\lambda, \text{Å}$	$H_S, \text{с}$	$H_N, \text{с}$	$F_S - F_N,$ с:сек	$\bar{H}, \text{с}$	F_S/F_N	λ_S/λ_N	π_S/π_N	$F_N(N)/F_N(S)$	$F_S(N) : F_N(N) :$ $F_S(S) : F_N(S)$
1 S	24.I 1965 г.	5250	2,66	4,53	-450	-1,67	0,42	0,54	0,92	0,474	1,4 : 0,5 : 0,4 : 1
1 N			4,54	3,72	+241	+0,96	2,90	1,31	1,31		
2 S	12.II	5250	2,42	3,29	-100	-0,42	0,97	0,83	0,86	1,17	1,6 : 1,2 : 1 : 1
2 N			2,84	3,48	-117	-0,34	1,36	0,79	1,42		
3 S	15.III	5250	3,26	4,94	-519	-1,40	0,30	0,58	0,69	0,650	0,7 : 0,7 : 0,3 : 1
3 N			4,32	4,13	-7	-0,09	0,97	0,92	1,00		
4 S ₉	15.III	5250	3,85	5,09	-965	-0,75	0,56	0,77	0,80	0,772	1 : 0,8 : 0,6 : 1
4 N ₉			5,16	5,32	+148	+0,35	1,30	0,98	1,02		
5 S	16.III	5250	5,20	6,22	+46	+0,026	1,07	1,12	1,00	0,745	1,7 : 0,7 : 1 : 1
5 N			6,28	5,43	+1330	+1,29	2,33	1,32	1,11		
6 S ₉	16.III	5250	4,66	4,45	+1055	+0,60	1,82	1,07	1,08	1,10	1,6 : 1,1 : 1,8 : 1
6 N ₉			5,43	5,08	+732	+0,35	1,41	1,18	1,06		
7 S	17.III	5250	3,36	5,31	-409	-1,72	0,48	0,66	0,69	0,302	3,4 : 0,3 : 0,5 : 1
7 N			6,10	3,82	+462	+1,99	11,20	1,61	1,98		
8 S	7.IV	5250	3,96	5,68	-1630	-1,43	0,43	0,63	0,94	0,94	0,6 : 0,9 : 0,4 : 1
8 N			5,44	5,99	-1350	-0,79	0,64	0,71	0,93		
9 S ₉	7.IV	5250	6,53	7,03	-1330	-0,83	0,70	0,87	0,92	0,93	0,8 : 0,9 : 0,7 : 1
9 N ₉			6,84	6,24	-3,3	-0,017	0,92	0,86	0,93		
10 S	15.VI	5250	3,64	6,17	-947	-2,07	0,20	0,40	0,60	0,532	0,4 : 0,5 : 0,2 : 1
10 N			4,15	3,94	-219	-0,47	0,68	0,69	0,80		

Table 6 (Continued)

№ п/п	Дата	$\lambda, \text{Å}$	H_S, sc	H_N, sc	$F_S - F_N,$ <i>sc-cek</i>	\bar{H}, sc	F_S/F_N	λ_S/λ_N	n_S/n_N	$F_N(N)/F_N(S)$	$F_S(N) : F_N(N) :$ $: F_S(S) : F_N(S)$
11 S	10.VII	5250	4,80	4,94	+203	+0,79	2,10	1,70	1,04	0,212	3,2:0,2:2,1:1
11 N			8,42	3,01	+1100	+4,38	14,9	5,13	1,69		
12 S	23.VII	5250	3,24	3,09	-86	-0,35	0,91	0,93	0,84	0,226	4,2:0,2:0,9:1
12 N			5,10	2,50	+630	+2,62	18,8	3,48	1,68		
13 S	24.VII1965г.	5250	3,14	3,42	-137	-0,58	0,62	0,68	0,97	0,310	2,2:0,3:0,6:1
13 N			5,23	2,63	+460	+1,93	7,02	1,91	1,43		
14 S	27.VII	5250	8,17	9,11	-1500	-1,46	0,57	0,76	0,75	0,700	1,0:0,7:0,6:1
14 N			11,02	8,99	+580	+0,60	1,40	1,03	1,09		
15 S ₉	27.VII	5250	9,37	11,2	-1250	-0,80	0,78	0,78	0,92	0,950	0,7:1,0:0,8:1
15 N ₈			9,56	9,35	-1390	-0,92	0,72	0,76	0,86		
16 S	29.VII	5250	2,67	3,08	-111	-0,47	0,67	0,79	0,95	0,753	1,5:0,8:0,7:1
16 N			4,18	2,65	+68,5	+0,27	1,96	1,06	1,00		
17 S	31.VII	6103	1,39	2,65	-105	-0,40	0,63	0,99	0,87	0,174	4,5:0,2:0,6:1
17 N			2,96	1,54	+322	+1,31	26,0	2,46	3,07		
18 S	1.VIII	6103	1,86	2,22	-86	-0,36	0,60	0,79	0,89	0,200	3,2:0,2:0,6:1
18 N			3,65	1,61	+437	+1,83	16,2	2,80	2,37		
19 S	2.VIII	6103	2,98	2,81	-554	-0,49	0,54	0,70	0,78	1,07	1,7:1,1:0,5:1
19 N			3,14	3,02	-286	-0,06	1,61	1,01	0,93		
20 S ₉	2.VIII	6103	2,88	3,19	-92	-0,06	0,98	1,02	1,02	1,01	2,4:1:1:1
20 N ₈			4,10	3,49	+1008	+0,34	2,36	1,05	1,03		
21 S	10.VIII	5250	1,89	2,76	-159	-0,70	0,30	0,57	0,69	0,413	1,8:0,4:0,3:1
21 N			3,61	1,54	+171	+0,66	4,27	1,19	1,46		
22 S	11.VIII	5250	1,30	1,95	-41	-0,19	3,70	1,39	0,88	0,311	6,1:0,3:3,7:1
22 N			2,99	1,14	+290	+1,20	19,5	2,64	1,70		

Table 6 (continued)

23 S	12.VIII	5250	6,36	3,69	+202	+0,80	2,03	1,03	1,00		
23 N			7,85	4,00	+420	+1,76	4,91	1,54	1,68	0,707	3,4:0,7:2,0:1
24 S	5.IX	5250	3,18	5,69	-282	-1,22	0,61	0,80	0,83		
24 N			5,54	3,57	+470	+1,93	10,3	2,59	2,14	0,240	2,4:0,3:0,6:1
25 S	20.IX	5250	2,31	2,60	+20	+0,084	1,38	1,10	0,90		
25 N			2,56	3,00	-3	-0,017	1,82	0,96	1,39	1,18	2,2:1,2:1,4:1
26 S	27.IX 1965 r.	5250	3,05	2,81	+37	+0,15	1,82	1,09	0,97		
26 N			3,13	2,44	+150	+0,62	2,40	1,15	1,39	0,638	1,5:0,8:1,8:1
27 S	17.X	5250	3,89	2,34	+373	+1,59	7,14	1,77	2,69		
27 N			4,09	1,89	+505	+2,12	24,3	2,34	3,37	0,585	14,2:0,7:7,1:1
23 S	30.XI	5250	3,16	2,67	+181	+0,75	4,32	1,96	1,99		
28 N			3,93	2,56	+433	+1,83	9,00	2,49	1,65	0,805	7,2:0,8:4,3:1
29 S	4.XII	5250	3,28	3,29	+98	+0,43	2,14	1,14	1,22		
29 N			4,03	2,68	+398	+1,64	4,45	1,67	1,64	0,495	2,2:0,5:2,1:1
30 S	13.III 1966r.	6103	5,17	7,91	-1009	-0,57					
30 N			6,06	8,48	-229	-0,17					
31 S ₉	13.III	6103	8,05	11,2	-463	-0,27					
31 N ₉			8,33	10,8	-825	-0,72					
32 S	13.III	5250	5,27	4,34	-473	-0,44					
32 N			6,53	6,87	-481	-0,33					
33 S ₉	13.III	5250	5,14	5,71	-358	-0,24					
33 N ₉			6,11	6,74	-519	-0,35					

completely renewed, i.e., would almost complete a cycle, after 24 hours, which would undoubtedly cause rapid (on the order of 24 hours) fluctuations in the mean value of the net field in a fixed section (with respect to the disk image). If the fluctuations in question were related to rotation, then the lapse at the N-polar region with respect to the S-polar region would be possible if some type of common magnetic anomaly passed straight along the solar meridian and, due to inclination in the axis of revolution of the Sun, extended to the north-south line, at the end of which our region is located, this meridian would, it seems, traverse the S-region earlier than the N-region (when the inclination of the N end of the axis of revolution is toward the eastern limb of the disk). However, the positioned angle of the axis of revolution from the end of July to the beginning of August, 1965, was close to zero, and in March, almost 20° ; so in the S-region, the traversal, conversely, should be later; hence, this effect could hardly be attributed to inclination in the axis of revolution of the sun. Moreover, localization of a magnetic anomaly strictly along the meridian from one pole to another is highly improbable. Furthermore, recordings for March 15 and 16, covering the entire disk and encompassing a wide range of latitudes (from the pole to $\pm 20 - 30^{\circ}$) and longitudes from the E to the W limbs of the Sun, does not confirm the rotation effect. Emissions introduced from new regions, emanating from the E limb, would hardly cause such fluctuation, because the increase in area due to rotation would be no more than 2%.

And finally, let us review the effect of selection, viz., that the values H and δH in fig. 11 and in table 6 were obtained by averaging fluxes and maximum amplitudes of sections which varied from day to day: For example, when the whole disk was recorded, these values encompassed a range from 30 to 70° latitude (S, N 1 - 8), while polar region recording covered, as a rule, the range 50 - 70° (S, N 0.5 - 3.0); moreover, the polar regions were recorded at 30" intervals, whereas the whole disk, at 60" intervals (See table 1). It follows from the discussion in Art. 2, that the heterogeneous selection of sections must lead to variations in magnetic flux values, i.e., to variations in the magnitude δH ; but in cases of chaotic distribution of the field, the effect of the choice of sections on the magnitude of δH is not essential - it varies in equal measure with the number of cases. Therefore, the periods which are of interest to us (first, the 15 - 17 March; and second, 23 July - 2 August), which show rapid fluctuations, were revised so that the choice of sections was the same throughout the entire period: there were 5 for the first period (S, N 1.0; 2.0; 3.0; 4.0 and 5.0) and for the second (S, N 1.0; 1.5; 2.0; 2.5). The results of working this data into a form that is more suitable for review than fig. 11 is given in fig. 12, which gives an original treatment of the data from fig. 11 and table 6.

A comparison of both results shows that, although selection has a marked effect on fluctuation and "amplitudes," i.e., lowering some peaks and raising others, it does not qualitatively change the picture:

for the second period the fluctuation effect and the shift in δH for peak II increased (in intensity); the effect (of selection) on H and δH increased for peak III; and the effect for a small peak at the S-pole, peak IV disappeared in δH , but increased in \bar{H} , and here the maxima of IV are synchronous. For points of the second period, the selection factor does not play a role.

The reality of synchronous field fluctuations at the N- and S-poles based on other data would be an extremely desirable verification. With this in view, we have employed several magnetic field maps of Mount Wilson Observatory¹, which contain information on the polar field (e.g., cf. Fig. 8). Unfortunately, due to the low resolution (23" X 23"), the maps contain information only on the largest elements of a relatively strong field (beginning at 3 gs per Mount Wilson calibration), and in a number of cases, do not give recordings of the polar field at all (due to a drop in sensitivity by a factor of 1.5 - 2.0 at the limb of the disk and the absence of a brightness compensator). From all the material (from March to November, 1965) only 21 days could be selected where the measurements were free from the following discrepancies: a) zero drift and field manifestations actually of only one sign both at the poles and over the whole disk; b) very scant data at the poles (late time of registration, clouds, etc.) and c) interference from clouds, adjustments, et al. For reasons which cause information loss at low resolution, see Art. 2. By isogauss planimetry in the polar zones (from 0 to N_6 , S_6 or over a latitude from

¹We are grateful to Dr. R. Howard (Mount Wilson Observatory) for placing these maps at our disposal.

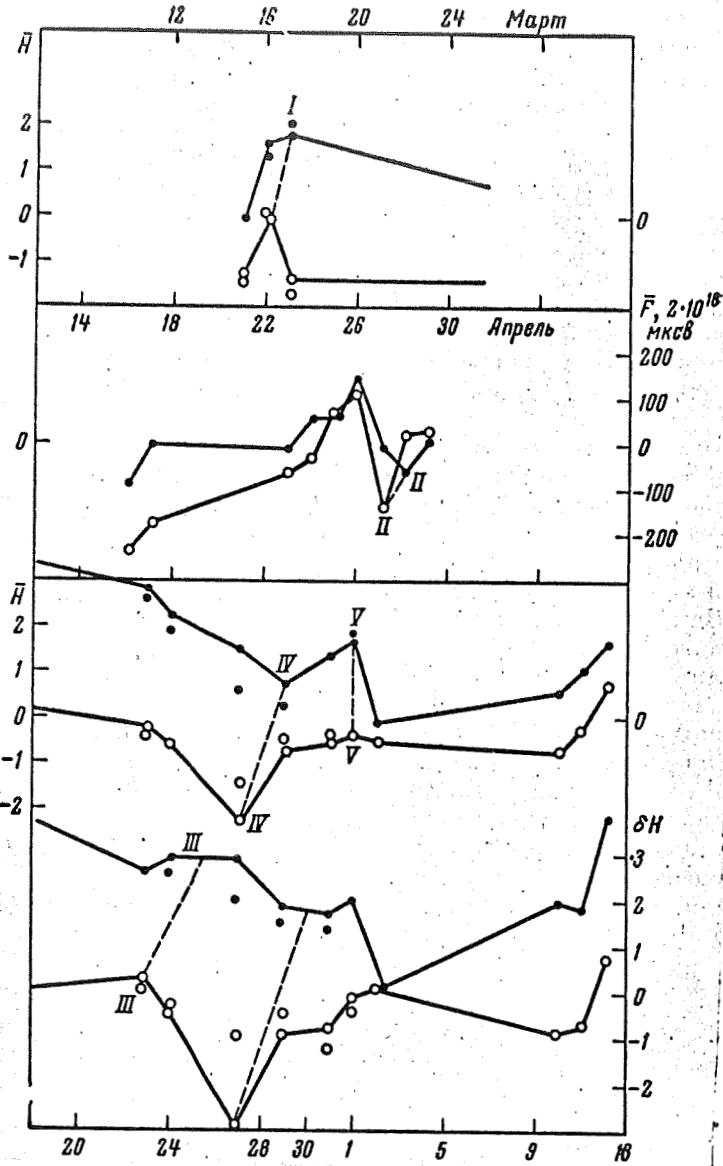


Fig. 12: Polar field fluctuations at the N-pole (dots) and S-pole (circles) as per measurements of the same sections of the polar cap (solid line): these same measurements affected by the selection effect (Fig. 11 and Table 6) are the points and circles not joined by a line.

90 - 56°), S- and N-polarity fluxes and the difference $F_S - F_N$, converted to Mx.v, were found. They are indicated in Fig. 11a by points and circles with dashes above them. A number of consecutive (day to night) data (from 22 to 30 April) show the same synchronous, rapid fluctuation of the polar field with a staggered minimum at the N-pole (28 April) relative to the minimum at the S-pole (27 April) (here, maximum magnitudes are the same--26 April). Regardless of the fact that the rapid synchronous fluctuations ("jerks" as it were) of the polar field seem

convincing, further research into possible explanations for the effect are necessary.

A second remarkable anomaly is protracted field variations: in the first half-year (February-June) the appearance of a field of the same negative sign was observed at both poles; while at the end of the year (September-December), the wave of a positive field was distinctly recorded at both poles. We see that the overwhelming majority of Mount Wilson data, which compensates deficiencies in our data for 1 October to 30 November, also shows this field rotation at the S-pole, i.e., at times, judging from the polar field, the Sun acts as a "monopole" of first one sign and then the other. At different periods, the fields disappear or drop to a low magnitude at one pole or the other (or both, 20 September, 1965). At the end of 1964, and in January and particularly July - August, 1965, the Sun acted as a "dipole."¹

If we now compare the balance of magnetic fluxes at the poles (for this purpose Table 6 gives values for $F_N(N)/F_S(S)$, the ratio of N-polarity fluxes at the N-pole to fluxes at the S-pole, and the ratio of fluxes in the last column of Table 6) then the average of fluxes for the whole year presents the following picture:

$$F_S(N) : F_N(N) : F_S(S) : F_N(S) = 3,2 : 0,6 : 1,5 : 1 \quad (3.4)$$

whereas, for the period from January to September, this ratio is 2:0:0.6:0.7:1, i.e., the appearance of a net S-field at both poles

¹It is easily verified, using the value H for the North $H(N)$ and south $H(S)$ poles (Table 6), that the difference $\bar{H}(N) - H(S)$ (net polar field of the Sun) is positive throughout the year and shows no seasonal advance with the heliocentric latitude of the Earth, B_0 , of the type found in [2].

at the end of the year sharply increases the imbalance of fluxes at the poles, which is characteristic of the whole year. If we compare this ratio with that measured in 1964,

$$2:0.5:1:1,$$

then it is apparent that the "magnetic asymmetry" of the Sun, in the sense that there is a predominance of uncompensated S-polarity flux at the N-pole, was maintained, although N-polarity flux in the southern hemisphere increased by a factor of ~ 1.5 .

It may be assumed that the magnetic asymmetry and other phenomena described above are only characteristic of the photosphere of the Sun, but in the upper strata, the picture for some reason "normalizes." Let us examine this problem. Measuring the general magnetic field in the chromosphere, in line $H\alpha$, is fraught with great difficulties. First is the low sensitivity of the H line to the magnetic field: the splitting of $\Delta\lambda_H \sim g\lambda^2$ is here 1.66 times less if the multicomponent picture in $H\alpha$ is compared to the normal triplet. The noise histogram (without a modulator) gives, for the weighted mean average of noise amplitude, $\bar{h} = 4.31$ gs, while in lines $\lambda\lambda 6103$ and 5250 it is about 2 gs[1]. This magnitude not only compares with intensity values characteristic of the general field (cf. Table 7) but also exceeds them, as the field intensity histogram shows. Moreover, protracted noise fluctuations have a mean "wave length" of 6.3" comparable to the characteristic length of small field elements, which also masks their appearance.

Table 7: Comparison of Photosphere and Chromosphere Fields (H)

Data	Pole	Линия	F_S , вс.м.м	F_N , вс.м.м	$\left(\frac{\text{фот.}}{\text{хром.}}\right)_S$	$\left(\frac{\text{фот.}}{\text{хром.}}\right)_N$	\bar{H} , вс	$\bar{\lambda}_S$	$\bar{\lambda}_N$	$\left(\frac{\text{фот.}}{\text{хром.}}\right)_S$	$\left(\frac{\text{фот.}}{\text{хром.}}\right)_N$
Дата, 1965 г.	Полус	Line									
23.VII	S	H $_{\alpha}$	54	185			-1,10	5,70	7,70		
		5250	89	193	1,64	1,04	-0,82	7,59	11,1	1,33	1,43
	N	H $_{\alpha}$	196	46			+1,27	12,8	5,93		
		5250	342	22	1,74	0,45	+2,65	18,0	4,17	1,40	0,70
24.VII	S	H $_{\alpha}$	82	162			-0,67	5,88	10,3		
		5250	109	174	1,33	1,07	-0,56	5,87	8,72	1,00	0,85
	N	H $_{\alpha}$	261	101			+1,23	10,9	7,62		
		5250	312	47	1,19	0,46	+2,28	12,9	6,24	1,18	0,81
31.VII	S	H $_{\alpha}$	40	142			-0,94	6,87	11,1		
		6103	62	98	1,56	0,69	-0,27	9,65	9,63	1,41	0,87
		6103	222	11,5	1,45	0,34	+1,15	10,6	6,33	1,29	0,65
	N	H $_{\alpha}$	153	34			+1,15	10,6	6,33		
		6103	222	11,5	1,45	0,34	+1,60	13,7	4,13		
		6103	222	11,5	1,45	0,34	+1,60	13,7	4,13	1,29	0,65
Среднее Average					1,48	0,68				1,27	0,88

A second reason is the strong effect of instrumental polarization on the zero position for recordings in H $_{\alpha}$ (see Table 2 and Fig. 1); here, the effect of zero shift reaches 1 - 2 gs in a good case; actually zero shift is difficult to eliminate due to the high intensity of scattered light (intense spectrum brightness of order I). Also, manifestations of H $_{\alpha}$ -line polarization are not to be excluded, since "quasiresonance" lines [10] constitute almost 3 - 5% in the event of prominences.

Finally, recordings of the whole field in H $_{\alpha}$ may be subject to the marked effect of both the ragged, filamentary make-up of this line due to the discrete structure of the chromosphere and the irregular velocities of its constituent fibers and also, due to the effect of emission formation in the chromosphere, which lead to the same asymmetric effect. In order to determine how much these factors affected the recordings, the same sections were registered in H $_{\alpha}$ with the ADP

polarization modulator shut off, which made possible the identification of those field fluctuations causing line profile asymmetry. Moreover, brightness in the body (and sometimes the wing) of $H\alpha$ was recorded simultaneously, which allowed for verification without $H\alpha$ emission affecting signal magnitude.

Of all the 1965 $H\alpha$ -line recordings, there were only three, which were selected and carefully analyzed, in which the majority of fluctuations could be related to true fields. Since $H\alpha$ and metallic line recordings during this period were at different times, then a comparison of individual sections would not be entirely accurate; it is better in this case, to compare the mean field for the whole polar region. The results of such comparison are given in Table 7.

We see that the signs of the net field \bar{H} in $H\alpha$ and the metallic line correspond in every instance: \bar{H} magnitudes show good agreement, also. Most characteristic, however, are the measured S- and N-polarity flux magnitudes F_S and F_N (or the mean intensities \bar{H}_S and \bar{H}_N , which were obtained by dividing F_S and F_N by 125 mm). In all cases, the southern field flux in the photosphere exceeded chromosphere flux by an average factor of 1 - 5. Noise effects show up in $H\alpha$ for the north polarity and are especially strong at the N-pole where the field of this polarity is weak--mean \bar{H} is considerably less than 1 gs (which is only 25% of the mean noise amplitude of ~ 4 gs). Regardless of this effect, the mean ratio of N-polarity fluxes in the photosphere and chromosphere show a total 30% deviation from unity. Apparently, it is a fact that S-elements (components) in the photosphere are larger

by 30% than in the chromosphere; however, a similar difference may be attributed to some small zero displacement in H-polarity H α recordings.

The most important conclusion to be drawn from comparing the polar fields in the photosphere and the chromosphere is that there is no essential difference in them, with the exclusion of intensity magnitude which, probably, is ~ 1.5 times greater in the photosphere. Hence, the characteristic disruption of flux balance (magnetic "asymmetry") found at the photosphere level of the field remains in force in the chromosphere. An analogous field asymmetry effect at the N- and S-poles in 1963 was found in [11] from polarization measurements of several chromospheric lines at the limb.

4. General Magnetic Field of the Entire Solar Disk

Fig. 13 gives examples of original recordings of the field for the entire disk for 27 July and 2 August, 1965, along with Ca^+ spectroheliograms for the same days. The good correspondence between the local fields and even weak fluctuations in Fig. 13 were mentioned more than once, earlier.

Looking at Table 6, the mean values for the polar and equatorial zones, in cases of recording the field of the whole disk, show that, for the southern hemisphere, the sign of the net field of the polar ($30 - 70^\circ$ latitude) and equatorial ($0 - 30^\circ$) zones were the same in 6 out of 7 cases, but there was no such correspondence in the northern hemisphere in 3 cases, the signs at the pole and at the equator were different, and in 4 cases, similar. In the southern hemisphere, the numerical values of the net field \bar{H} of the polar and equatorial zones showed good correspondence to each other, while in the northern hemisphere there was no such correspondence. The magnetic field of the southern hemisphere was substantially more uniform in magnitude and sign, which, in most cases, was negative (N-polarity). At the same time, great inhomogeneities in the sign of the field were observed in the northern hemisphere; this is also apparent from the distribution of flux $F_S - F_S$ with latitude (See below Fig. 14; 16 March, 1965, is an exception for the southern hemisphere). These peculiarities also express the unique "magnetic asymmetry" of both hemispheres of the Sun, cited in [1] based on 1964 measurements. This was especially strongly expressed, apparently, from September

to December, 1965, when the sign of the mean field H at the S-pole became positive--the same as at the N-pole (Fig. 11). It is difficult to not relate this magnetic asymmetry to the sharply expressed asymmetry of solar activity: the overwhelming majority of active zones in 1964 - 1965 were concentrated in the northern hemisphere, including here, the distribution and intensity of green and red coronal emissions, which is well illustrated in bulletins of the Boulder High Altitude Observatory [12].

A more detailed presentation is given by the graph in Fig. 14 which shows the distribution, by latitudes, of net magnetic flux magnitudes $\Delta F = F_S - F_N$ (3.3), averaged over all latitudes at each longitude for which a section was made. We see here, for example, the distributions for March 15 and 16 when rapid variations in the mean net field of the polar regions took place: April 7, when the field at both poles was negative; July 27 (a polar field of various signs); and August 2, when the field had a "dipole" character. There is obviously no type of regular flux change ΔF with latitude, but, on the contrary, irregular and sometimes rapid changes of sign and flux magnitude are observed. However, all distributions have in common, a predominance of negative flux (N-polarity) and an irregular magnetic distribution in the southern hemisphere, including the pole. In the southern hemisphere in 4 out of 5 cases the following similarity may be observed: the presence of 2 zones with a rotating field--zones of negative field: one at the equator ($\varphi = 20^\circ$) and the other in the median latitudes ($\varphi = 35 - 50^\circ$). Upon comparing the distributions

Fig. 13: Recording of the general field of the whole disk and spectroheliograms for 27 July, 1965, (a) and 2 August, 1965 (b).

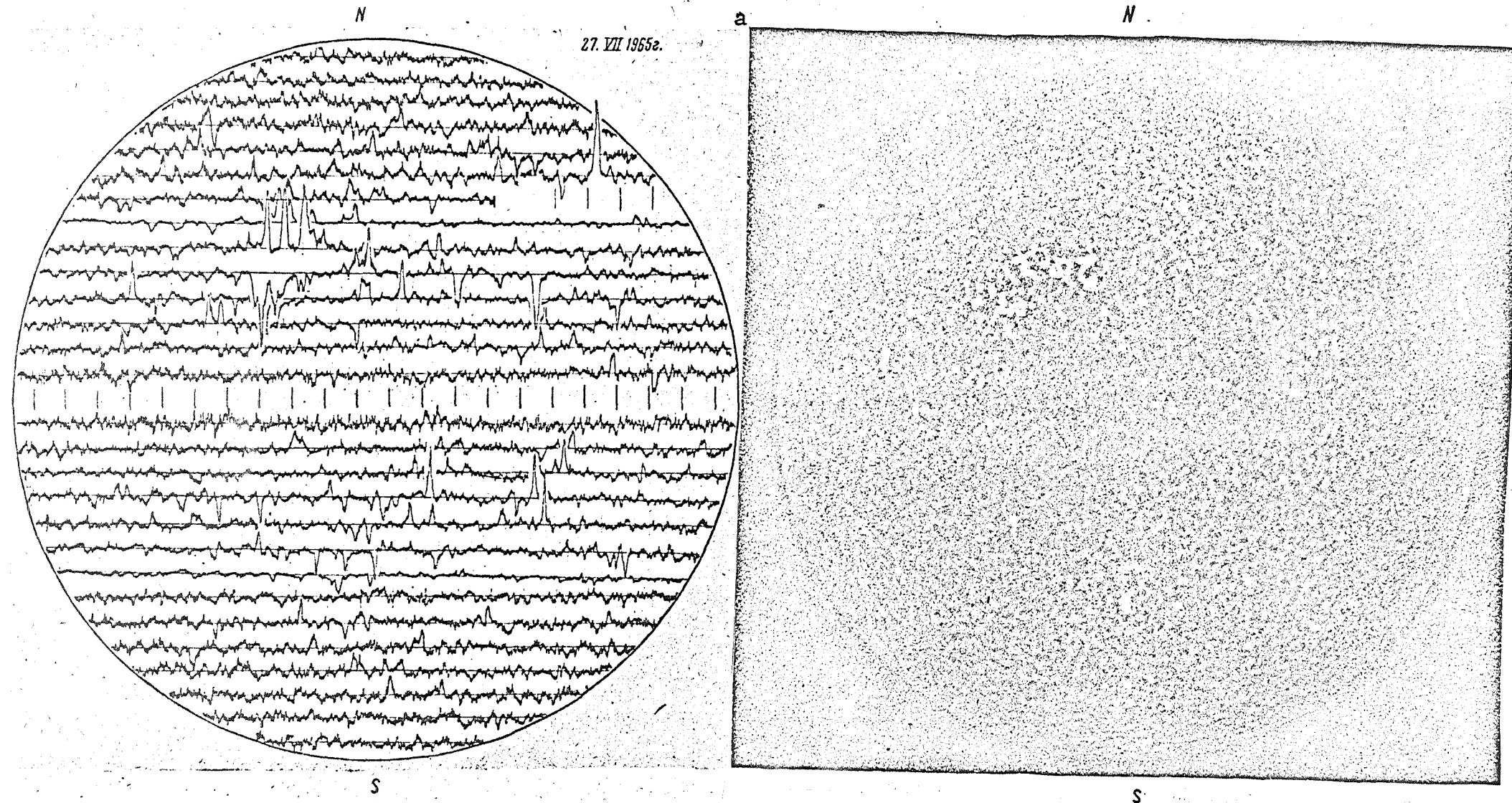
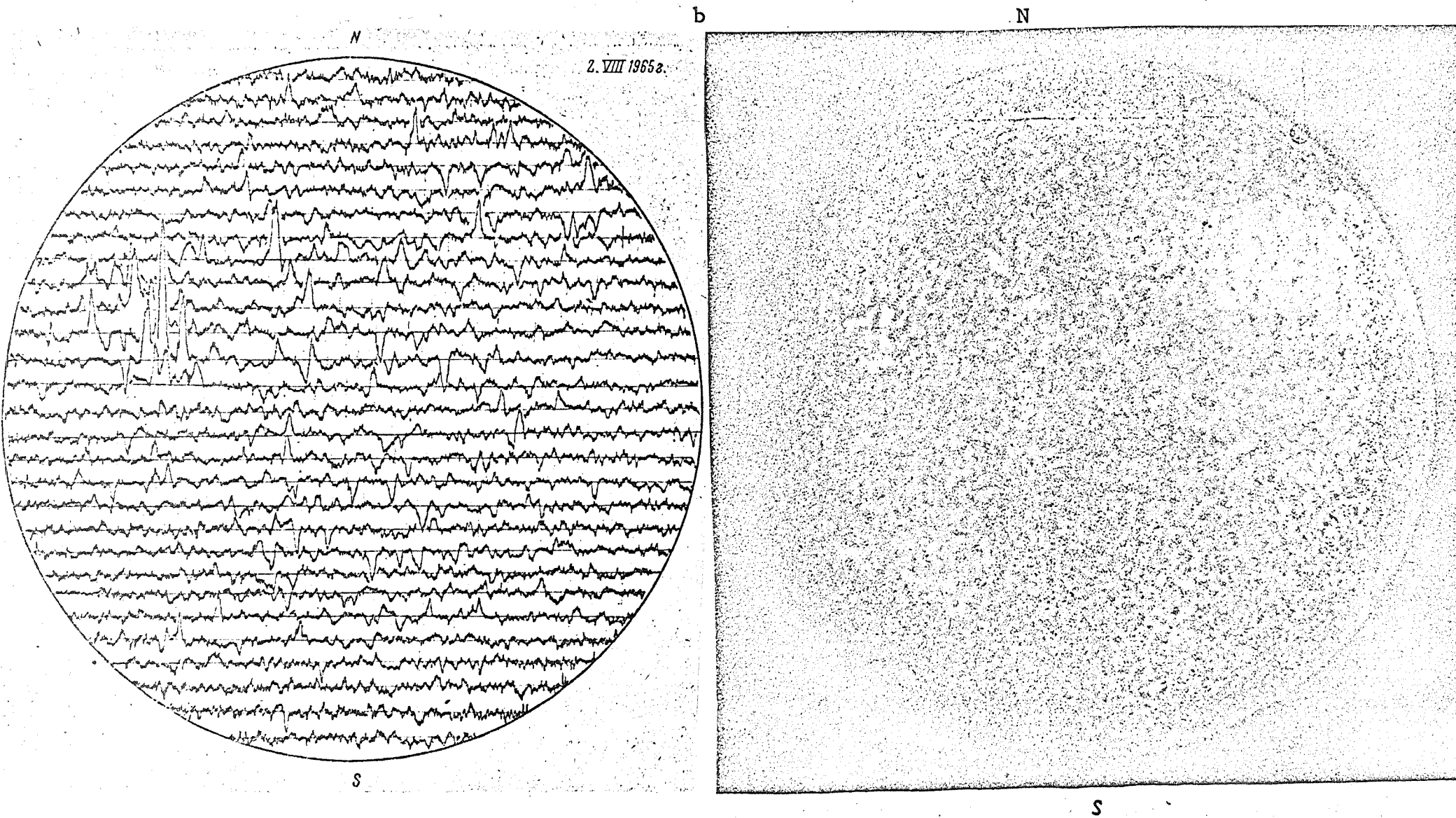


Fig. 13 (continued)



of March 15 and 16 (Fig. 14), it is possible to find some similarity between them: all the peaks for the 16th (I, II etc.) are somewhat shifted towards the equator in relationship to their position on the 15th (if sign is ignored). If our predication of peaks for all dates is correct, then we obtain the following magnitudes of magnetic disturbance "shifts" toward the equator and their velocities (counting a time interval equal to 10^5 sec).

Пик Peak	$\Delta\phi$	$R_{\odot} \Delta\phi, 10^3 \text{ км}$	Скорость, км/сек Velocity km/sec
I	+14°	1,75	1,75
II	+16	1,95	1,95
III	+21	2,56	2,56
IV	+9	1,10	1,10
V	+3	0,35	0,35
VI	+15	1,80	1,80
Average			1,58 км/сек.

A velocity of 1.6 km/sec is characteristic of photospheric movements. If, in the given case, we actually have a systematic drift of characteristic field disturbances from the poles to the equator (along the meridian), then this could be connected with the well known theoretical phenomenon of meridional circulation--the radial outburst of gases at the poles and their flow towards the equator along the meridian [13]. True, these movements proceed much slower, Therefore, if the velocities of magnetic disturbance, as found in Art. 3 and also evaluated here, reflect a true process, then they should, more than likely, belong to disturbances of the fluctuation or wave-type which run from one pole to the other. It is appropriate to remember that Alvin's wave velocity in the photosphere (in a ~ 10 gs field) is of the same order, ~ 1 km/sec (or a bit less).

It is immediately apparent that on March 15, an exemplary balance of fluxes was observed in the northern hemisphere, but in the southern hemisphere, the S-polarity field is practically nil, so that the total net flux from the whole Sun is negative; whereas, on March 16, the total flux is positive in both hemispheres. In the remaining cases, the net field is negative. This may seem strange, when one considers the predominance of an average S-polar field at the poles, as follows from Table 6 and (3.4). However, a review of this table shows no such S-polarity dominance for the days studied. Secondly, the fluxes in this Table belong to the polar zone, whereas, here we are dealing with an integral over the whole disk (the predominance of S-polarity at the N-pole may be "masked" by emanations from the other part of the disk). Finally, the fluxes $F_S - F_N$ in Table 6, Art. 3 were computed on the basis of mean field strength in a definite section, and in the given case we are comparing integrals from this magnitude on the basis of latitude (see below, Table 8). Correcting for zero position, calibration, etc., showed that the flux magnitude F_S from the 15th to the 16th of March was an actual effect; it follows, also, to keep in view, that the recording for 15 March is incompletely evaluated: data on the equatorial zone are lacking, as this was an instance when the majority of emissions from the southern field occurred March 16th. The lifetime of the individual field components as cited by us in [14] is from 4 - 10^h, so that after 24 hours, the general field is essentially renewed.

Let us now review the relationship between true field flux

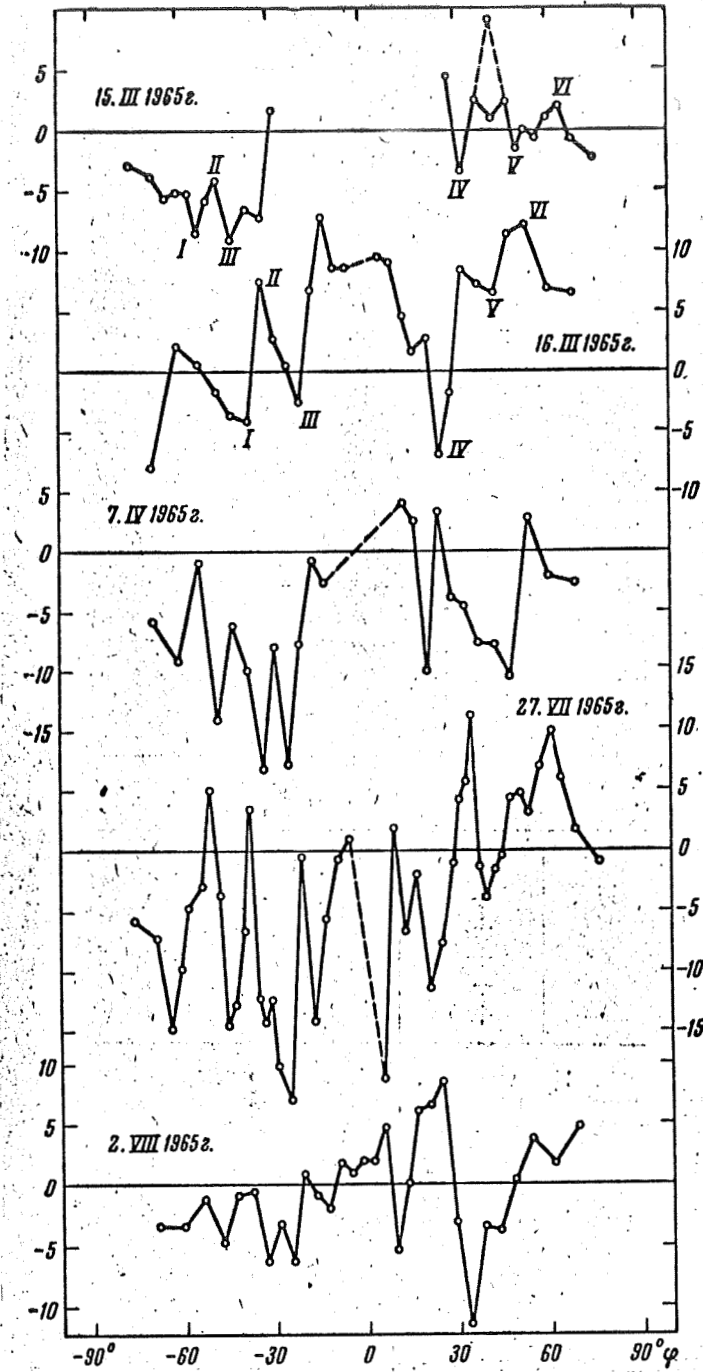


Fig. 14: Distribution of mean flux $F_S - F_N$ (for a given latitude) of the general magnetic field for different recordings of the general field: The values for $(F_S - F_N) \cdot 10^{-21} \text{ Mx}\cdot\text{v}$ lie along the vertical axes. The dashed lines for the 15 March, 1965, recordings indicate cases when a spot was included in determining the difference $F_S - F_N$.

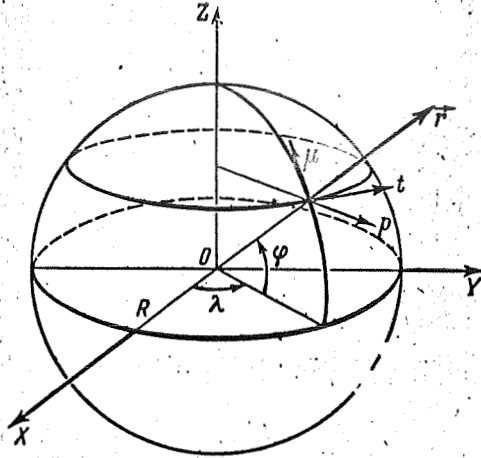


Fig. 15: On the determination of a relationship between total and measured flux.

through the visible hemisphere of the Sun

$$F_0 = \iint H_R d\sigma = R^2 \int_{-\pi/2}^{+\pi/2} \int_{-\pi/2}^{+\pi/2} H_R \cos \varphi d\varphi d\lambda \quad (4.1)$$

and the magnitude measured by us (3.3)

$$F_{S,N} = \int_0^L H_{||} dl = R \cos \varphi \int_{-\pi/2}^{+\pi/2} H_{||} \cos \lambda d\lambda \quad (4.2)$$

Here (Fig. 15), it is obvious that

$$dl = R \cos \varphi \cos \lambda d\lambda, \quad (4.3)$$

where φ is latitude, λ is the longitude of points on the surface of the sun, and the axis x is taken in the direction of the line of sight, so that $H_{||} = H_x$; and H_R is the radial component of the field vector. It is apparent that

$$\begin{aligned} H_R = (H, r_1) &= H_x \cos \varphi \cos \lambda + H_y \cos \varphi \sin \lambda + H_z \sin \varphi = \\ &= H_{||} \cos \varphi \cos \lambda + H_{\perp} (\cos \chi \cos \varphi \sin \lambda + \sin \chi \sin \varphi), \end{aligned} \quad (4.4)$$

Here H_{\perp} is the lateral component of the field constituting angle χ with axis y . From equations (4.1) and 4.2) on the strength of (4.4)

it follows that

$$F_0 = F_{||} + F_{\perp}, \quad F_{||} = R \int_{-\pi/2}^{+\pi/2} F_{S,N} \cos \varphi d\varphi, \quad (4.5)$$

Table 8: Total Flux of the General Magnetic Field of the Sun as a Whole.

Дата Data	K	Hemisphere						$F_{\parallel} \cdot 10^{21} \text{ Mx.v}$	$H_{\odot}, \text{ gc}$
		N-полушфера			S-полушфера				
		F_{+}	F_{-}	$F(N)$	F_{+}	F_{-}	$F(S)$		
1 15.III	4,90	356	163	+193	8,6	2680	-2670	-2480	-0,163
2 16.III	4,75	5650	386	+5260	3490	780	+2710	+7970	+0,525
3 7.IV	4,72	715	2610	-1900	12,9	6000	-5990	-7880	-0,518
4 27.VII	4,04	1790	3760	-1970	120	6980	-6860	-8860	-0,582
5 2.VIII	4,32	1980	1630	+ 350	276	1790	-1510	-1160	-0,0765

Remarks by Number

- 1) Incomplete recording. No equatorial zone flow is calculated without spots (group 76); with $M F_{\parallel} = -1.70 \cdot 10^{21} \text{ Mx.v}$. By Mount Wilson data, flow $-1.88 \cdot 10^{21}$.
- 2) Reliable value; Mount Wilson data for 3.16 unavailable; for the 17th they are noted as unreliable. S-fields partially non-existent.
- 3) Mount Wilson Data is unavailable.
- 4) Mount Wilson Data is unavailable; for 7.28 this data are marked as unreliable--notes recorded very late, fields in polar zones absent.
- 5) Mount Wilson data is noted as unreliable due to strong electronic variations: zero drift to the N-pole is noted (in the S direction of S-polarity).

i.e., total flux is derived from the flux F_{\parallel} , connected with measurements by us of the "flux" of the longitudinal component, and the flux F_{\perp} from the lateral component. Strictly speaking, in order to determine the complete flux in a general case, it is necessary to know not only H_{\parallel} but also H_{\perp} . The magnitude F_{\parallel} , thus, may be determined from observations, knowing $F_S - F_N$, (fig. 14), and multiplying them by $\cos\varphi$ and integrating over φ . In order to express it in Mx.v, it must be taken into consideration that F_{SN} is expressed in gs, multiplied by mm of length of the recording. Table 8 gives the cost of 1 mm of recording in seconds of arc on the Sun (this is determined by recording speed and scale); if F_{SN} is expressed by the number of gs multiplied by the number of sec of arc, then obviously the unit

$$F_{S,N} = R \cdot (\text{length in cm}) = 6,95 \cdot 10^{10} \cdot 7,70 \cdot 10^7 = 4,95 \cdot 10^{18}.$$

The fluxes of S(+) and N(-) polarity (in Mx.v) for each hemisphere were computed by planimetry from the distribution $F_{S,N} \cos\varphi$ for each day (Table 8); here (Table 8) net fluxes for both hemispheres and for the Sun in general, F_{\parallel} , are given. We see that the total flux of the longitudinal field varies from $+8 \cdot 10^{21}$ to $-9 \cdot 10^{21}$ Mx.v, that is, takes on both positive and negative values, attaining values which exceed the field flux from large spots ($\ll 8 \cdot 10^{21}$ Mx.v [15]). This flux variation is equivalent to the mean variation

$$\bar{H}_{\odot} = \frac{F_{011}}{\pi R_{\odot}^2}$$

within the limits of -0.5 to +0.5 gs, which characterizes the behavior of the Sun as a magnetic variable star.

In order to evaluate the extent to which the flux fluctuation F_{\parallel} , found by us, affects the total flux variation F_0 , the emanation from (contribution of) F_{\perp} must be found. Let us introduce at each point on the sphere (R, φ, λ) the orthogonal coordinate system (r, μ, t) with the origin at this point, with the axis r along the radius vector of points where μ is the tangent to the meridian, and where t is tangent to the circle of latitude at this point. Let $\{H_r, H_{\mu}, H_t\}$ be the vector components of field H at the point (R, φ, λ) in this system. From Fig. 15, we have

$$\left. \begin{aligned} H_x &= H_{\mu} \cos \varphi + H_t \sin \varphi, \\ H_y &= H_{\mu} \sin \varphi - H_t \cos \varphi, \\ H_z &= H_r \cos \lambda = H_r \cos \varphi \sin \lambda - H_{\mu} \sin \varphi \sin \lambda + H_t \cos \lambda, \end{aligned} \right\} \quad (4.6)$$

so that

$$F_{\perp} = \iint \left\{ H_r (\sin^2 \varphi + \cos^2 \varphi \sin^2 \lambda) + H_{\mu} \sin \varphi \cos \varphi \cos^2 \lambda + H_t \cos \varphi \sin \lambda \cos \lambda \right\} d\sigma. \quad (4.7)$$

Let us evaluate this magnitude for the case of a dipole field. In this case we have

$$\left. \begin{aligned} H_r &= H_m \sin \varphi, \\ H_{\mu} &= -\frac{1}{2} H_m \cos \varphi, \\ H_t &= 0, \end{aligned} \right\} \quad (4.8)$$

where $H_m = 2a/R^3$ is the dipole moment. In this case, (4.1) and (4.7) are easily calculated, and we obtain

$$F_{\perp} = 2\pi R^2 H_m, \quad F_{\perp} = \frac{2}{3} \pi R^2 H_m \approx \frac{1}{3} F_0, \quad (4.9)$$

i.e., a large part (about 70%) of the flux F_0 is determined by the magnitude of F_{\perp} , since the variations in this magnitude characterize variations in total flux. In other cases, without knowing the specific

distribution of the field, it is difficult to give a reliable evaluation of the emanation of (i.e., the contribution of) F_{\perp} .

It follows to mention that the disruption of the balance of S- and N-fluxes for the entire disk is on the whole (for the days shown in Table 8), equally applicable to the poles is a fact which is related, as already cited in [1], not to transformations in field strength, but to transformations in areas and to the dimensions of the components of the predominant polarity. This is well illustrated in Fig. 16, which shows the distribution of the average ratios \bar{H}_S/\bar{H}_N and \bar{L}_S/\bar{L}_N for a given latitude over the whole disk: regardless of the high, overall predominance of \bar{H}_S over \bar{H}_N ; in all cases the ratio \bar{L}_S/\bar{L}_N is considerably less than unity, which also leads to the predominance of $F_N \sim \bar{H}_N \bar{L}_N$ over F_S . This indicates that the mean gradient

$$\left(\frac{\partial H}{\partial x}\right)_N > \left(\frac{\partial H}{\partial x}\right)_S, \quad (4.10)$$

since the S components are more lengthy but the intensity is not strongly different, that is, the forces acting on N components are greater than the forces acting on S components.

Variation in the magnitude and sign of the net flux (or mean intensity) of a field in the visible hemisphere of the Sun has a direct bearing on the problem of magnetic variable stars. Our registrations indicate comparatively rapid fluctuations in the mean poloical field, which are very difficult, if not impossible, to explain by the rotation effect: the absence of a field at the S-pole in the first half of 1964, the appearance of a field of one sign at both poles from September - October, 1965, the occurrence of rapid

(almost 24 hr) synchronous fluctuations, and other facts, do not support the rotor hypothesis. Data on the general field of the Sun is still scant, but the data given in this paragraph show that fluctuations in the sign and magnitude of the total flux are entirely actual and are characteristic, not only for the polar field, but also for the whole general field, as already cited by us in [1] and [16]. Recently, a report [17] on rapid fluctuations (5 times in several days) of net magnetic flux, according to data from magnetic maps of Mount Wilson (within the range of $\pm 60^\circ$ from the center of the disk), for revolutions 1431 - 1437, was issued; it was also found that the flux for this period remained negative (in the sense that $F_N > F_S$). Unfortunately, due to information losses of approximately 50% of all field components at a resolution of 23" X 23" (see end of Art II) and the occasional appearance of a field of only one sign on the map (zero drift), it is difficult to say to what extent these measurements represent actual fluctuations in the flux of the general field, but apparently, some of them are real (perhaps the text dealt with only those cases when there were no spots on the disk); spots are not admissible in flux determination.¹ In one way or another, a careful study of the general magnetic field of the sun from the point of view of explaining the rapid fluctuations in flux is of great interest in understanding the nature of the magnetic variability of stars and Sun.

¹It should be kept in mind that one spot may give a flux equal to the total flux of the general field of the sun.

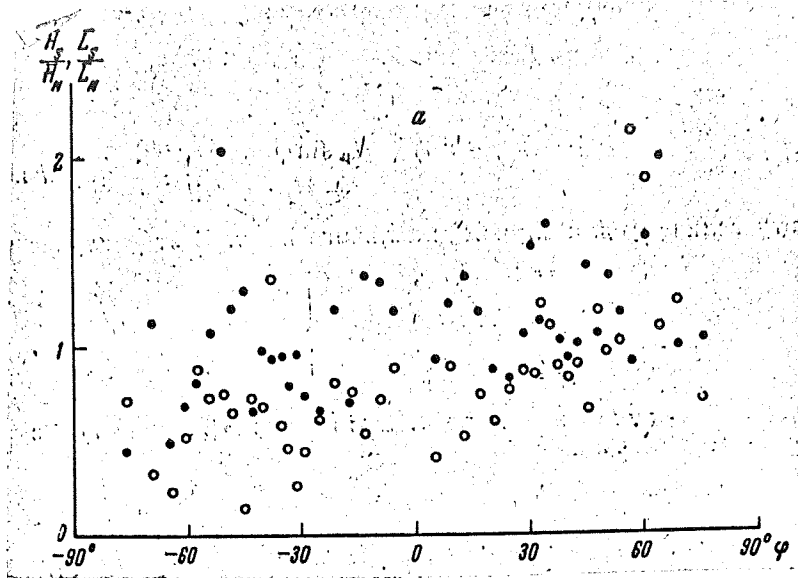


Fig. 16: Example of the distribution of the ratios \bar{H}_S/\bar{H}_N (dots) and \bar{L}_S/\bar{L}_N (circles) according to latitude for 27 July, 1965, recordings of the general field.

5. Auto-Correlation of Field Fluctuations and Cross

Correlation of Field-Velocity:

Dimensions of Magnetic Non-uniformities

Determination of the correlation between neighboring deviations (autocorrelation) in recordings of a field (or radial velocity) permits a determination of to what extent flux fluctuations in recordings differ from actual cases. The range of actual difference of the coefficient of autocorrelation from zero depends on the characteristic dimensions of the magnetic components. If u_i, u_{i+m} is the deviation from the arithmetic mean value (in a series of measured deviations of the recording), then the coefficient of auto correlation [15] is

$$r_m = \frac{n}{n-m} \sum_{i=1}^{n-m} u_i u_{i+m} / \sum_{i=1}^n u_i^2, \quad (5.1)$$

Where m is the order of autocorrelation ($m = 1$ gives the correlation between neighboring members of the series; and $m = 2$, the same for all members over 1, etc.). If the fluctuations form a very long, homogenous series, then, according to the increase in m , we may divide the series so that the number of measured points for any m will always be the same, equal to N ; then instead of (5.1) we have

$$r_m = \frac{\sum_{i=1}^N u_i u_{i+m}}{\sum_{i=1}^N u_i^2} \quad (5.2)$$

The length of the recording of the field divided by $N = 150/300$ equidistant points; an interval between the points is usually from 0.5 to 1.0 mm, or from 1.5" to 3" (on the disk of the Sun). Computation was carried to $m = 30$ on the computer.¹ Autocorrelation curves (A.K.) are shown in Fig. 17, un-normalized ($\sum_{i=1}^N u_i u_{i+m}$, above), and normalized (5.2) (below) for a series or a number of recordings: averages of 10 such curves for 10 sections of recordings of the field--in the center of the disk (Sec. 240" X 240") for 14 November, 1964 (in line 5250), on the average of 2 curves for 2 long recordings polar field (from the W limb to the E limb) for the N- and S-poles, 13 March, 1965, were made simultaneously, both for the line λ 5250 and also for the line λ 6103. Recordings were carried out at a resolution of 2.5" X 9", speed of 1"/sec and time constant of 2.5^s. In this same Figure 17, squares indicate the autocorrelation for fluctuation in the intensity of the calcium spectroheliograms obtained in [19]. Regardless of the change in contrast and size in the cells of the calcium grid with the cycle of cell activity [20], our autocorrelation

¹The author expresses his gratitude to N. V. Godovnikov for compiling the program and calculating the autocorrelation curves on the computer "MINSK-1" and to G. Ya. Vasil'yeva for counsel on questions connected with the application of correlation analysis.

shows good agreement with the autocorrelation for the calcium grids measured in 1953; at the same time, autocorrelation [21] for field fluctuations, recorded with a very small aperture (2.5" X 2") show substantial deviation from all of these data (circles); analogous correlations [21] were obtained also in [22] with a large aperture (2.4" X 6"). We see that, regardless of essential difference (Fig. 17) in autocorrelation (in absolute units) for the center of the Sun (triangles) and the poles and also for the N-pole (crosses, large values) and the S-pole (points, small values), the relative autocorrelations (Fig. 17) are practically the same if one does not consider the rise in the total curve due to the effect of a small, constant mean field (at the distance $\sim 30''$) in two cases. This does not indicate also an essential difference in the relative autocorrelation of the different lines in which the recording is made. This is extremely important, because both lines control each other independently. The agreement between $\lambda 5250$ and $\lambda 6103$ is entirely valid since these lines are close to each other in depth of image [4]. Somewhat unexpected, are the high (absolute) values of r_m expressed in gs^2 . It is further obvious that the large r values of $r_m gs^2$ for the N-pole (than for the S-pole) express the magnetic asymmetry effect of the polar field mentioned above.

The good correspondence between our autocorrelations and those in [19] expresses the well known fact of a very tight correlation between magnetic fields and the calcium chromosphere grid, both as to position and also in the sense of the correspondence of intensity and

brightness (the latest data on this may be seen in [23] and [24]). Power spectra for the averaged curve (from the autocorrelations given in Fig. 17), give in all but two cases, a constant field at the 30" section, are given in Fig. 18 and were computed on the computer and were calculated on the computer according to the formula

$$E(k) = \frac{2}{\pi} \int_0^{\infty} r_m \cos kr dr, \quad (5.3)$$

which shows nothing new in comparison with [2], unless perhaps a small maximum for the characteristic length of $5.2'' = 4,000$ km.

Let us review the effect on magnetic field recordings of such distorting factors as photomultiplier noise and image fluctuation. At a high time constant, fluctuation noise (Schottky effect) of long "period" may be mistakenly accepted as real field fluctuation, especially with small apertures, when the noises are comparable to the signal from the general field. Vibrations lead to the rapid appearance and disappearance of the range of a high or low (and even a reverse sign bias) field, which, during constant scanning, are recorded as field fluctuations. This effect is more strongly expressed at small apertures because they are comparable to the vibration amplitude. In order to explain the role of these disturbances, we made recordings at different resolutions and time constants τ of both the "pure" noises of the PEM (photoelectricmultiplier) (with the polarization modulator off), and also noises connected with image vibration and PEM noises. In this case, the image of the Sun was not scanned, but held in a fixed position in the slit of the spectrograph and recordings on EPP-09 were made at a speed at which magnetic fields are usually

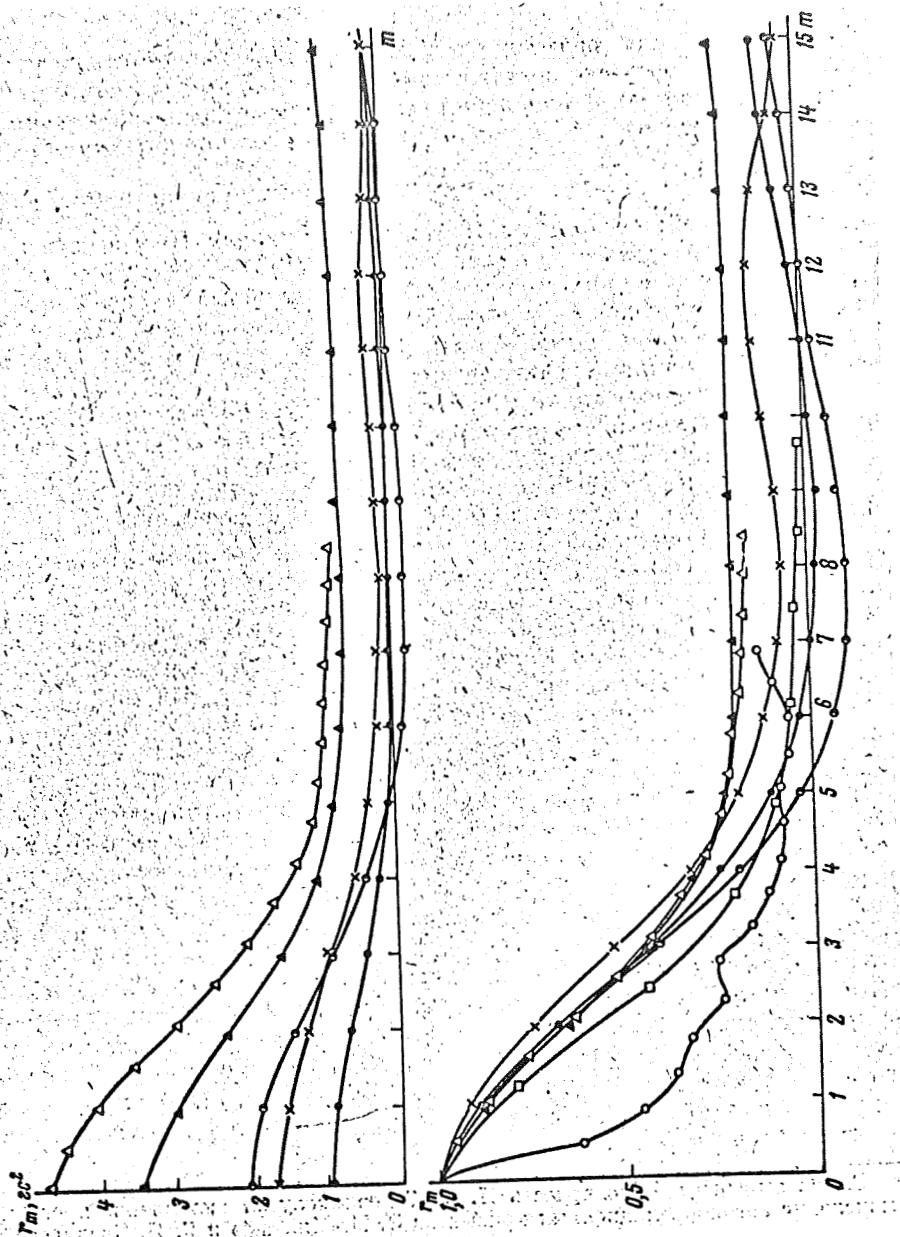


Fig. 17: Autocorrelation curves of magnetic field fluctuation, unnormalized (left) and normalized (right) (5.2) for 10 recordings at the center of the Sun, 14 Nov., 1964 (average open triangles); and two long sections of the polar zone recorded 13 March, 1965, in λ 5250 (dots, S-pole; crosses, N-pole) and simultaneously recorded in λ 6103 (half-darkened dots and darkened (closed) triangles for the S- and N-poles, respectively). Unit length along axis x equals 2.85.

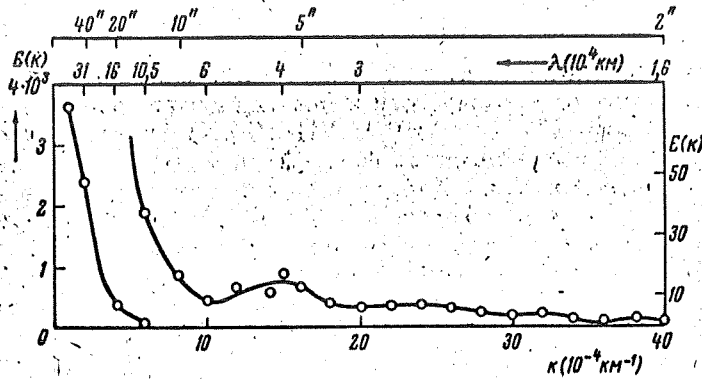


Fig. 18: Power spectrum for mean autocorrelation curve of Fig. 17: below the wave numbers $k = 2\pi/\lambda$, where λ is the characteristic dimension (above, in km and sec/arc) .

recorded ($1''$ per 1^s , $v = 30$, and $1''$ per 2^s , $v = 60$). All of the fluctuations recorded in this way would then be caused apparently by image fluctuation and PEM noises. Table 9 gives data on these measurements, and Fig. 19 gives autocorrelations for each set of data.

The autocorrelations for noises collected in Fig. 19 show serious differences which apparently, in the majority of them, are related to the presence or absence of a fluctuating magnetic field area, near the aperture, with a fluctuation amplitude which gives an autocorrelation, or nearly so, with the recording of an actual field distribution, or something different from this (the latter). The autocorrelation of only single noises also strongly affects the transparency and the time constant of the recordings (compare the two recordings) made without an ADP, 13 July and 14 November, 1964). Upon comparing these noise autocorrelations with those in Fig. 17, we see that the effect of noise may be significant. As for example: the normalized autocorrelations [21] [22] completely, as is not

Table 9: Noise Recordings

Дата, 1964 г. Data	Модулятор Modulator	τ , сек	ν	R	$r_m(0)$, вс^2	Обозначения на Фиг. 19 Designation in Fig. 19.
13.VII	Off Выключен	2,5	30	2"5x9"	2,5	1
13.XI	On Включен	5,0	30	2"5x9"	2,2	2
14.XI	Off Выключен	5,0	60	2"5x8"	2,62	3
23.XI	On Включен	2,5	30	1"5x5"1	15,8	4
28.XI	"	5,0	30	1"5x5"1	7,5	5

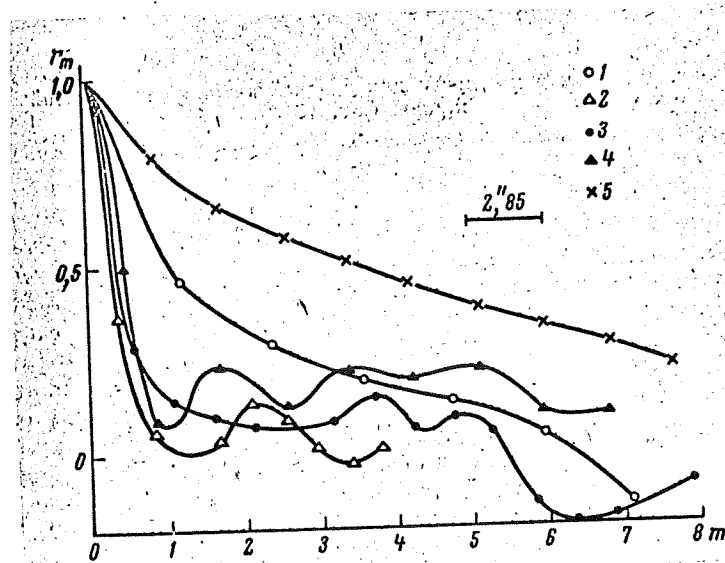


Fig. 19: Autocorrelation curves of longitudinal field signed fluctuation in terms of image fluctuations and PEM/photomultiplier/noise (cf. Table 9 for designations).

difficult to prove, lie within the range of noise autocorrelations in Fig. 19. Since for "noise" autocorrelations sometimes reach noise values comparable with those of ordinary field recordings (Fig. 17), the discrimination of noise fluctuations connected with vibration is no simple matter. It would be extremely beneficial to investigate this problem in detail, although the conclusions would hardly agree with those in [25], because the autocorrelation of these spectra characterize more so, the "carrying" capability of the method of registration than the fine structured fluctuations themselves (granulation, the general field).

At an average distance of $r_m = 0.5$, the field fluctuation of 13 Marcy, 1966, reached 7.7" for our autocorrelations, although for individual autocorrelations, it fluctuated from 7.1" to 9.2"; for 14 November, 1964, this value reached 7.5"; the stated values are close to the integral value of autocorrelation

$$\int_0^{\infty} r_m dm = 6", 8.$$

A drop in autocorrelation to zero may be considered to take place at a distance of $\sim 20"$. A small, secondary maximum is possible at 30", but its appearance is not always discernible. Not to be excluded is the possibility, finally, that the scale of autocorrelation for actual field fluctuations changes from case to case, reaching 5.5"¹ or even lesser values, as stated in [21] and [22]; however, in this case the effect of noise is amplified and very unreliable.

¹The value found by G. Ya. Vasil'yeva for our 13 July, 1964, recording of the field.

Table 10: Histogram of Magnetic Component Lengths

l	Pole N-ПОЛЮС		Pole S-ПОЛЮС		Equator N-ЭКВАТОР		Equator S-ЭКВАТОР	
	S	N	S		S	N	S	N
0-4"	61	94	71	61	9	19	21	11
4-8	207	203	269	209	67	44	71	65
8-12	261	235	280	231	70	58	63	71
12-16	310	274	283	293	98	102	100	111
16-20	185	138	149	194	75	72	81	90
20-24	205	130	175	211	90	86	98	82
24-28	139	121	106	151	70	87	59	86
28-32	89	88	73	109	50	53	57	57
32-36	71	65	58	81	46	47	48	34
36-40	63	52	42	69	40	42	35	38
40-44	46	38	21	39	16	32	25	21
44-48	48	35	31	47	27	32	21	28
48-52	21	22	16	30	14	16	11	19
Сумма... Total	1706	1495	1574	1725	672	693	690	713

Of interest also is the distribution of "wave lengths" of the fluctuation of the general magnetic field of S- and N-polarities, determined from the statistical distribution of lengths of S- and N-components on the recordings, themselves (Art. III). Histograms of the lengths of S- and N-components for both fields, and also for the equatorial zones to the N- and S- of the equator (in the case of recording the whole disk), were constructed for each date shown in Table II. They do not show any type of systematic difference with time, therefore, in Table X and Fig. 20, we have given summary histograms for the whole of 1965 of the S and N deviations for both poles (top) and the equator (bottom). Their comparison does not show serious differences: for the poles, there is a relatively small increase in the frequency of short components ($1 < 16''$) and a decrease in the frequency of long components ($1 > 20''$); this may be due in part to the influence of the projection effect. The predominance of average

length of S-components at the N-pole over the lengths of N-components, which is confirmed by the data in Table VI, is evident, from which it follows that the mean ratio $\bar{\lambda}_S/\bar{\lambda}_N = 1.86$ at the N-pole. For the S-pole, such a predominance of dimensions was not discovered, and from Table VI it follows that $\bar{\lambda}_S/\bar{\lambda}_N = 1.00$. Upon relating frequency distribution according to length [1] and confirming this distribution by the result of [26], the main maximum is concentrated in the interval of 8 - 16". Just as for analogous histograms for 1964, along with the principal maxima in the range 8 - 16", secondary maxima show up well in the interval 1 from 20 - 24", and a small frequency increase in the range of 44 - 48" is observed. The principal maximum corresponds well to the doubled radius of correlation 7.5"; from Table 10 it is apparent that, for the poles, this dimension is on the average of 62% and at the equator, 47%, that is, on an average of $\frac{1}{2}$ or a bit more of all of the total number of all magnetic components, which could be expected. The complete length of autocorrelation (about 20") corresponds well to the secondary maximum and the discontinuity in the distribution curve at $l \gtrsim 44 - 48"$ (about 35,000 km). This characteristic dimension corresponds to the mean dimension of a super granule, according to [27]. However, the number of magnetic components of this size is small, that is, no more than 10% of the general number. The secondary maximum for lengths 20 - 24" (17,000 km) appears only for magnetic components (about 25% of all components); it would be interesting to find the optical analogue since the dimensions of the Ca^+ cell of the chromosphere grid is always higher than this value-- it varies from 30 - 90,000 km [19, 24].

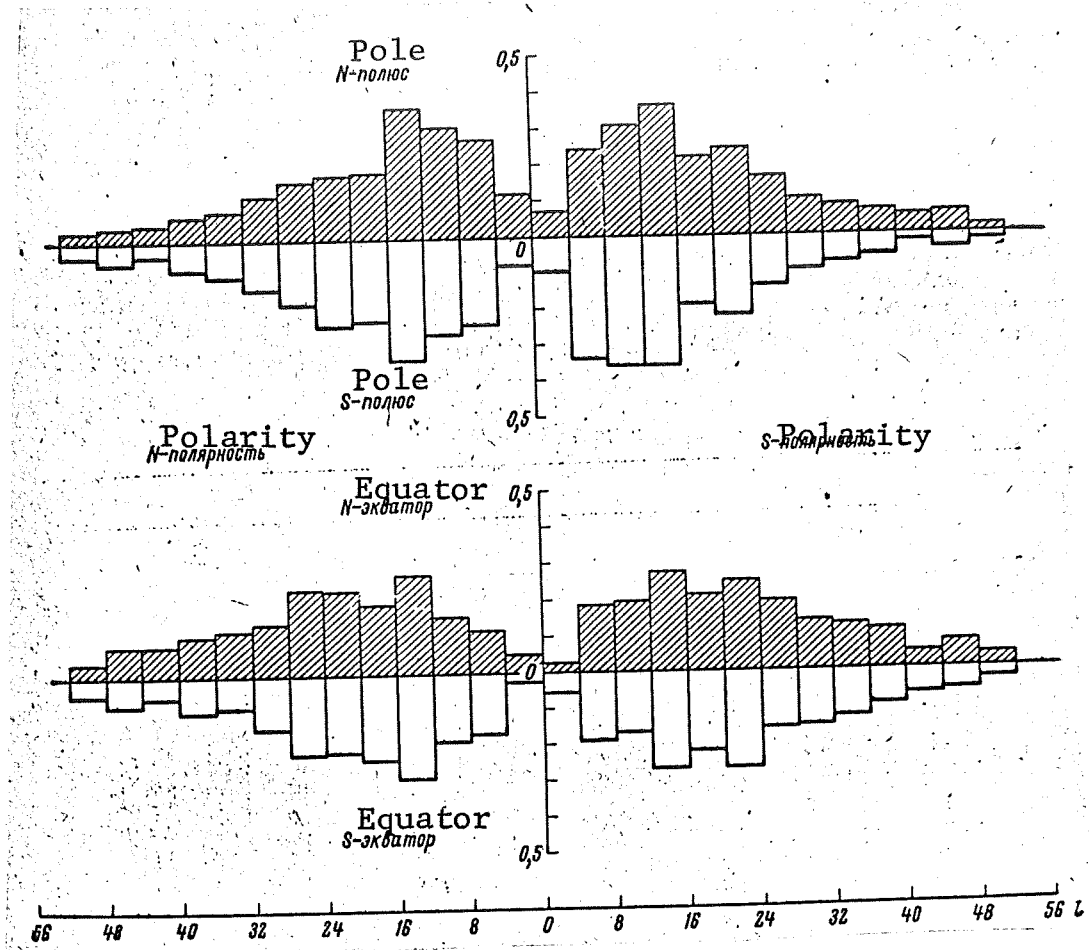


Fig. 20: Average histograms, for all of 1965, of general magnetic field component lengths at the N- and S-polar (upper) and equatorial zones to the N and S of the equator (lower).

The characteristic dimensions found by us, 12 - 16, 20 - 24, and 44 - 48", form a sequence, which is obtained by almost doubling the previous member, similar to the "overtones" of some stationary fluctuation state of a magnetized "liquid", as was mentioned by us in [1]. This brings about the idea of relating the general magnetic field to the field of a velocity which characterizes the motion of plasma on the surface of the Sun.

The following reasons indicate the possibility of relating field H and velocity. First, for a simple unidimensional radial tube of

lines of force, under the condition of suspended state, this relationship may be perceived from condition of preservation of state

$$SHv = \text{const}, \quad (5.4)$$

where S is the area of a section of the tube. Further, if we multiply the basic hydromagnetic equation for the accompanying liquid (rejecting the member with the extinguished field, since it exists only for large (on the order of a year) intervals of time)

$$\frac{\partial \mathbf{H}}{\partial t} = \text{rot}(\mathbf{v} \times \mathbf{H}).$$

by the quantity H in the same point, then, after averaging, we will obtain by time period

$$\frac{\partial \overline{H^2}}{\partial t} = \overline{H \cdot \text{rot}(\mathbf{v} \times \mathbf{H})}. \quad (5.5)$$

∏ and the turbulent scrambling of lines of force ordinarily lead to $\frac{\partial \overline{H^2}}{\partial t} > 0$, i.e., the right side of (5.5) is positive, and if $\overline{H} \neq 0$, then $\text{rot} \mathbf{v} \times \mathbf{H} \rightarrow \alpha^2$, that is, there must be some correlation between v and H.

To find the correlation between the longitudinal field H_{\parallel} and the velocity along the line of sight, we have used a recording of the entire field for 13 March, 1966, over the entire disk simultaneously at two levels of the solar atmosphere-- $\lambda 6103$ and $\lambda 5250$ (difference of level, ~ 260 km). Examples of these recordings are given in Fig. 21; for velocities, we have drawn a smooth median course from the W to the E limb of the disk and reviewed the fluctuation v_{\parallel} relative to this median. The interval was chosen just as in the case of autocorrelation, with a length of $\sim 300''$, back a bit from the limb of the disk, and divided into equidistant parts (at a distance of $2.85''$). According to the formula

$$k = \frac{\langle v_{\parallel} \rangle}{\sqrt{\langle H^2 \rangle \langle v^2 \rangle}}, \quad (5.6)$$

where

$$\langle vH \rangle = \frac{1}{L} \int_0^L H(x)v(x) dx, \langle v^2 \rangle = \frac{1}{L} \int_0^L v^2(x) dx, \langle H^2 \rangle = \frac{1}{L} \int_0^L H^2(x) dx, \quad (5.7)$$

we have calculated the coefficient of cross correlation. Directly from Fig. 1, it is apparent that there is a well expressed correlation between the recordings of the field at two levels; it is difficult to ascertain the presence of this type of relationship in the case of field-velocity, because the eyes notice a correlation even when $k \geq 0.5$. However, for velocities at two levels the correlation is also well expressed. Table 11 gives the results of calculations (on the computer, see Footnote 2) of the coefficient k for different sections (latitudes) across the disk of the Sun. We see that k , as a rule, is ≥ 0.5 for relationships between the fields separately and the velocities separately at two levels. However, for the correlation field-velocity, the magnitude k does not exceed 0.5 (in one case, 0.28). Besides this, we see from Fig. 17 that the coefficient of autocorrelation at a distance which corresponds to the difference in the level of $\lambda 6103$ and $\lambda 5250$ (300 km) always seems greater than the coefficient of a cross correlation between the fields; this indicates, even at a distance of ~ 300 km (diameter of a granule) a relationship between the fields which, in considerable measure, weakens and a large part of the general field being measured is concentrated in a very narrow stratum. The loss of relationship is still more strongly expressed in comparing recordings of H_{\parallel} in $\lambda 5250$ and H_{α} ¹.

The fact of an almost complete absence of correlation between

¹The author is grateful to Prof. M. Huber, Boulder, U.S.A. for useful counsel on questions concerning field-velocity during his visit to the observatory.

field and velocity is extremely difficult from a theoretical point of view, a fact that is noticeable even for the active regions of the Sun [28]. It is possible that, as a result of rapid fluctuations in velocity with the period of 290^s , as found in [3], this relationship is poorly expressed when registering fields that usually require much time. However, this problem requires more attention in the future.

6. Principal Results and Nature of the Magnetic Variability of the Sun

We have presented the indisputable fact of comparatively rapid fluctuations, during the course of a year, from season to season, of the general magnetic field of the Sun, during which the magnetic flux at both poles over the entire visible surface changes magnitude and sign, and particularly, in a manner in which the Sun in average formation changes from a magneto-unipole and becomes bipolar, and vice versa. We have observed the "magnetic asymmetry" of the N and S hemispheres--more often, a predominance of average S-polar magnetism in the Northern hemisphere, an effect which accompanies the asymmetry of solar activity. The fact of a visible disturbance in the mean balance of magnetic fluxes, both for polar zones and also for the entire visible hemisphere of the Sun, is a phenomenon characteristic apparently of the majority of magneto-variable stars. It is difficult to attribute this to the rotation effect; still, there are a few, but reliable, measurements which show that the re-establishment of a

balance of fluxes, which is observed at the photosphere level, can hardly be expected in the chromosphere. And also we can hardly expect it, apparently in the upper strata of the atmosphere, that is, in the corona or also in interplanetary space. A sector of the diagram of the interplanetary field, according to measurements from October, 1963, to February, 1964, at Interplanetary Station IMP-1, shows that the interplanetary field is very finely structured: its magnitude and sign changed rapidly, and the field of one sign appears, at most, 20% more often than the other [29]. If the interplanetary field is a continuation of the solar field, which shows a close connection between data on the planetary field and the appearance of a region of high magnetism on the Sun, then the fine structure of the interplanetary field is a reflection of the fine structure of the general field of the Sun, and the predominance of a field of one sign indicates a continuation of the effect of disturbance of balance, which is observed in the photosphere and the chromosphere, and in interplanetary space.

Along with this, very rapid (on the order of 24 hours) "synchronous" fluctuations have been discovered, i.e., "a lapse" of the polar field (possibly, the field as a whole) during which the peak values of the mean field at the N-pole lag behind these same values for the S-pole by 1 - 2 days, which requires a velocity of ~ 10 km/sec for the propagation of magnetic disturbance from pole to pole.

The nature of these rapid fluctuations and also the longer

fluctuations mentioned above, is not clear, as is the case of the magnetic variability of stars, which is "one of the most interesting and challenging problems of astrophysics" [30]. Most of all, it follows to note that purely magnetic fluctuations (of an incompressible ideal fluid) [31] would require internal fields of over 10^6 gs in order to give a period approaching that observed. If the studied effects are related actively to some type of solar fluctuations as a whole, then they must be, as correctly cited in [32], mechanical fluctuations (magnetic forces on the average are not large), their frequency would be $\sim GM/R^3$, and their period on the order of 2 hrs. The possibility of stationary, "standing" waves on the surface of the sun is indicated by a series of maxima in the frequency of occurrence of characteristic lengths of magnetic components, which form a series (12", 24", 48") of the overtone type; these maxima are not sharply expressed; which is, possibly, connected with the disturbance of the fluctuation state of convection and turbulence.

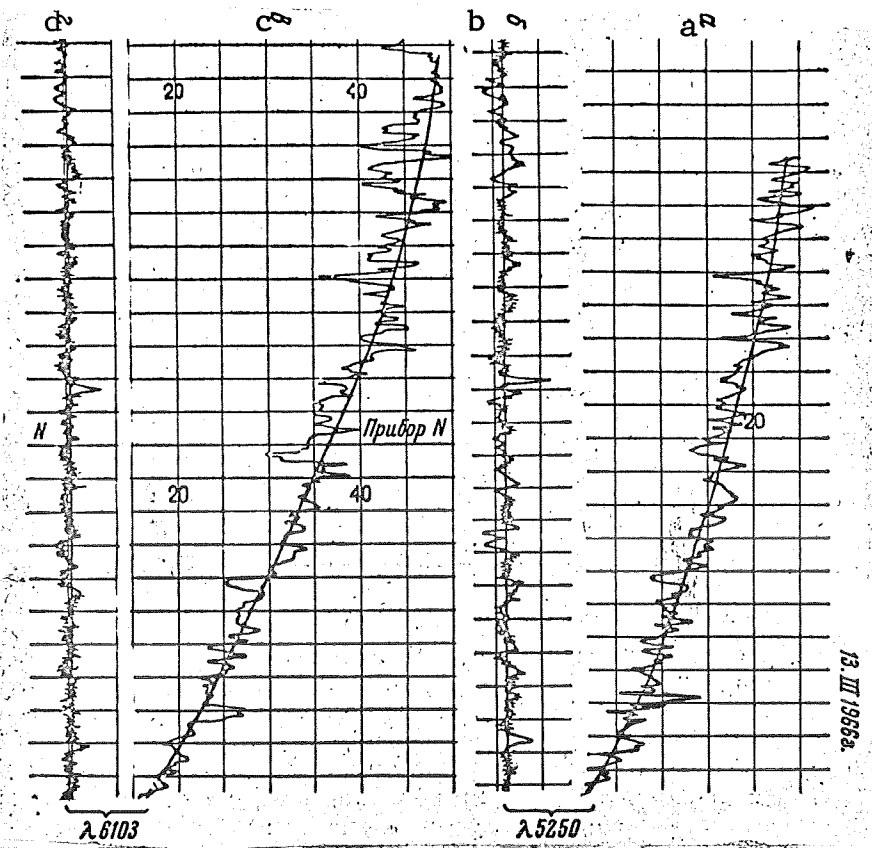


Fig. 21: Examples of simultaneous magnetic field recordings in 5250 and in 6103 (b and d) and radial velocities in these lines (a and c) obtained 13 March, 1966, upon recording the general magnetic field.

Table 11: Coefficients of Field-Field and Field-Velocity Cross Correlation for General Magnetic Field Recordings, 13 March, 1966

№ п/п	Кросс-корреляция Cross-correlation	φ^*			
		-53,8 S_1	+53,8 N_1	-42,7 S_2	+42,7 N_2
I	$\lambda 5250 : H_{\parallel} - v_{\parallel}$	0,012	0,159	—	-0,107
II	$\lambda 6103 : H_{\parallel} - v_{\parallel}$	-0,078	0,057	-0,051	-0,225
III	$\lambda 5250 H_{\parallel} - \lambda 6103 H_{\parallel}$	0,533	0,564	0,193	0,615
IV	$\lambda 5250 v_{\parallel} - \lambda 6103 v_{\parallel}$	0,587	0,288	—	0,610

№ п/п	Кросс-корреляция Cross-correlation	φ^*			
		-24,8 S_1	+24,8 N_1	-20,8 S_2	+20,8 N_2
I	$\lambda 5250 : H_{\parallel} - v_{\parallel}$	-0,193	0,029	0,157	-0,106
II	$\lambda 6103 : H_{\parallel} - v_{\parallel}$	-0,191	0,131	0,275	0,028
III	$\lambda 5250 H_{\parallel} - \lambda 6103 H_{\parallel}$	0,767	0,556	0,499	0,336
IV	$\lambda 5250 v_{\parallel} - \lambda 6103 v_{\parallel}$	0,508	0,495	0,429	0,559

In order to explain changes in the magnitude and sign of the field of the entire disk of the Sun, we might consider the motion of a type of gyrating fluctuation [2], when the surface layer moves, first faster, then slower than the internal layers, trailing off frozen "suspended" lines of force. This would lead to variations in the inclination of lines of force and possibly, to changes of sign. From this point of view, it would be interesting to trace the variations over the entire disk of the Sun, and also the time function of the shift effect of bright centers of the Ca^+ chromosphere grid and quiescences of the field in H_{α} relative to quiescences of the photospheric field. In [14] we found that on an average the former were shifted to the E (fell behind during rotation) relative to the latter, but this is an average effect: in individual cases, a shift to the

equator was observed. It is possible that the distribution of these shifts over the disk is different, and that they vary periodically with time. This mechanism, however, is not effective during "field suspension", as shown in [32]; the absence of field-velocity correlation favors the idea that fluctuations may, in a comparatively short time, change field during the emanation of lines of force, which, up to this time, lie over the surface. In line with this, it follows to mention that the emanation, apparently may be realized as a direct result of fluctuation, but not the "brilliance effect," which for the general field, is negligible, as shown in [33]. That rapid fluctuations of velocity with a period of 290^s actually take place at the surface of the Sun is an experimental fact, first described in [3].

Another possible manifestation, especially of rapid fluctuation, rises from the incongruity of the magnetic axis and the axis of rotation [30]. This was first rejected for the sun on the basis of earlier observations by Hale, which gave reason to believe that the magnetic axis corresponded with the axis of rotation. However, these observations are inadequate as a whole and scanty, as are all photographic measurements of the general field. The quantitative difference of the field from a dipolar field, the manifestation of an average field of one polarity at both poles and over the whole disk, the magnetic asymmetry of the N- and S-hemispheres, and other facts indicate that the concept that a permanent magnetic solar axis is not

logical (with the exception, perhaps, of brief intervals of time in 1965): If such an axis does exist, then its position in space, determined on the basis of symmetry of location relative to its magnetic "mass" on the surface of the Sun, by far would not correspond with the axis of rotation.

The other side of the problem is the statistical character of the general field, in particular, the absence of field-velocity correlation, which gives no basis for accepting the picture drawn in [34] that requires the concentration of a field in the limbs of a super granule, where a substance flows inside. The effect of such concentration in the limbs of convective vortices is theoretically impossible during the motion of a strongly flowing liquid across the field [35] (the flow effuses from the body of the cell). However, the autocorrelation curves and histograms found by us for field distributions magnetic component lengths do not show increases in frequency and dimensions characteristic of a super granule. They show substantially smaller dimensions, which is in good correspondence with the data in [19] for fluctuation in the intensity of the calcium chromosphere grid. Likewise, we didn't obtain any type of indication of a relationship between the components of a magnetic field and convective cells, i.e., granules. This may be related to the fact that at depths higher than h (the upper boundary of the convective zone) the motion is completely irregular (possibly, turbulences of a varying degree) not being related to convective motions below the

level of h , or depending on these motions only in that they are created by convection. In this case, the magnetic energy of chaotic fluctuations must be constricted, due to the massive scale (dimensions greater than the complete scale of autocorrelation) of the field components which are "pieces" of a field "chipped off" from the sun spots and which exist for a comparatively long time. It would be important to find evidence of the existence of such large scale fields in registrations of the general field.

In conclusion, the author expresses his gratitude to E. I. Limorenko for processing the recordings of the field, and to V. I. Gapeyev for preparing the final illustrations.

December, 1966

BIBLIOGRAPHY

1. А. Б. Северный. Астрон. ж., 1965, 42, № 2, 217; Изв. Крымской астрофиз. обс., 1966, 35, 97.
2. H. W. Babcock, H. D. Babcock. *Astrophys. J.*, 1955, 121, 349.
3. R. Leighton. *Astrophys. J.*, 1959, 130, 366.
4. А. Б. Северный. Астрон. ж., 1966, 43, № 3, 465.
5. D. Beggs, H. von Klüber. *Monthly Notices Roy. Astron. Soc.*, 1964, 127, 133.
6. А. Б. Северный. Изв. Крымской астрофиз. обс., 1963, 31, 163.
7. J. O. Stenflo. *Observatory*, 1966, 86, 73.
8. R. Howard. *Observatory*, 1966, 86, 162.
9. R. Howard. *Astrophys. J.*, 1959, 130, 193.
10. B. Lyot. *L'Astronomie*, 1937, 51, 217.
11. G. Brückner. *Zs. Astrophys.*, 1963, 58, 73; «Planetary and Stellar Magnetism», NATO Advanc. Study Inst. 26 Apr.—1 May 1965.
12. High Altitude Observatory, Rep. N HAO-62, Dec. 22, 1965.
13. К. де Ягер. Структура и динамика атмосферы Солнца. ИЛ, 1962, гл. 9, стр. 324.
14. A. Severny. *Trans. I. A. U.*, 1965, XIIA, 755.
15. W. Grotrian, H. Kunzel. *Zs. Astrophys.*, 1950, 28, 28.
16. A. Severny. *Colloq. Fine Struct. of the Solar Atmosph.*, Anacapri, June 6—8, 1966, edit. by K. O. Kiepenheuer, *Forschungsberichte* 12, p. 109.
17. V. Vumba, R. Howard, S. Smith. *Proc. Goddard Sympos. on Magn. Stars*, 1965, preprint.
18. Д. Э. Юл, М. Д. Кендал. Теория статистики. М., Госстатиздат, 1960, гл. 27, § 27—4.
19. J. Rogerson. *Astrophys. J.*, 1955, 121, 204.
20. Т. Т. Цап. *Наст. том*, стр. 92.
21. R. Howard. *Astrophys. J.*, 1962, 136, 211.
22. Г. Я. Васильева. Изв. ГАО, 1964, 23 (5), № 175, 28.
23. Т. Т. Цап. Изв. Крымской астрофиз. обс., 1965, 34, 296.
24. G. Simon, R. Leighton. *Astrophys. J.*, 1964, 140, 1120.
25. M. S. Uberoi. *Astrophys. J.*, 1955, 121, 406; 1955, 122, 466.
26. В. М. Григорьев, В. Е. Степанов. Сб. докл. по «Физике Солнца». Спб. ин-т земного магнетизма, ионосферы и распространения радиоволн. Иркутск, 1966.
27. R. Leighton, R. Noyes, G. Simon. *Astrophys. J.*, 1962, 135, 474.
28. С. И. Гопасюк. Изв. Крымской астрофиз. обс., 1966, 35, 139; 1967, 37, 29; *наст. том*, стр. 65.
29. N. Ness, J. Wilcox. *Science*, 1965, 148, № 3677, 1592; *J. Geophys. Res.*, 1965, 70, № 13.
30. L. Spitzer. *Electrom. phen. in cosmic phys.*, Symp. № 6. I. A. U., Cambridge, 1958, p. 169.
31. M. Schwarzschild. *Ann. d'Astrophys.*, 1949, 12, № 2, 148.
32. T. Cowling. *Monthly Notices Roy. Astron. Soc.*, 1952, 112, 527.
33. E. Parker. *Astrophys. J.*, 1955, 121, 491.
34. R. Leighton. *Annual Rev.*, 1963, 1, 19.
35. N. Weiss. *Planetary and Stellar Magnetism*, NATO Advanc. Study Inst. 26 Apr.—1 May 1965, in press.

13. K. de Yager. *Structure and Dynamics of the Solar Atmosphere, II Foreign Literature*, 1962, Ch. 9, p. 324.
18. D. E. Yul, M. D. Kendal. *Statistical Theory*, Moscow, State Publishing House, 1960, ch. 27, Art. 27 - 4.
20. Т. Т. Tsap, This volume, p. 92...26. V. M. Grigor'yev, V. Ye. Stepanov, *Collection of Reports on "Solar Physics."* Collections of the Institute for Terrestrial Magnetism, Ionospherics and Radio-wave Propagation. Irkutsk, 1966.